Charging of aerosol particles

An investigation of the possibility of using
Americium-241 for SMPS chargers

Sofie Hansen

2018

LUNDS
UNIVERSITET

Sofie Hansen
MVEM30 Examensarbete för masterexamen i miljövetenskap – Fördjupning i tillämpad klimatstrategi 30 hp, Lunds universitet
Intern handledare: Adam Kristensson, Avdelningen för kärnfysik, Fysiska institutionen, Lunds universitet
Biträdande handledare: Arash Gharibi, Avdelningen för ergonomi och aerosolteknologi, Institutionen för designvetenskaper, Lunds universitet

CEC - Centrum för miljö- och klimatforskning
Lunds universitet
Lund 2018

Ethical considerations and risk assessment

Beta and alpha-radioactive sources used in this study are giving ionizing radiation, which is harmful for humans. The intention of this report is to test it for an environmental application, and not for other means. The beta-emitting radioactive sources have been acquired from existing lab equipment from the aerosol lab at Lund University, while the alpha-emitting sources have been acquired from disposed smoke detectors. We strongly discourage the handling and acquiring of these radioactive sources, and it is forbidden to work with these radioactive sources without the involvement of radiation and safety personnel.

Before beginning the laboratory part of this thesis, a risk assessment was performed by authorized staff at Lunds University. It included a review of the fire exit, the restrictions both of the chemicals used, mostly butanol, and the different machines and instruments. Other circumstances about the laboratory environment was partly presented during this time, other special circumstances was reviewed during the time spent in the laboratory.

A specific review was made with the radioactive substances that can be obtained in the laboratory, which included its storage place and special safety prescriptions for these. It is important both for the university and author of this thesis that these safety prescriptions are followed with great care. The author never came closer than a few decimetres of the radioactive

substances. The assistant supervisor always handled the addition of new Americium radioactive sources (further called Am-sources) due to both the policy of the university but also since the author of this thesis did not attend courses about handling radioactive substances.

The risk assessment was signed by Sofie Hansen and Patrik Nilsson, Research engineer at the Division of Ergonomics and aerosol technology. It is also important to add that the author of this thesis was not alone in the laboratory for most of the time spent there. During the time when the author was alone, the fall-alarm was worn in all cases to make it possible for the guards to act if the person had fallen down.

Abstract

Climate change is a fact and effects everybody on this planet, whether its humans, plants or animals. There is a comprehensive agreement about the mechanisms on how aerosol particles affect the radiative balance of the earth, but there is a need of more knowledge to fully understand climate change and the strength of the aerosol radiative forcing.

The aim of this thesis is to investigate if the SMPS system can use a charger based on the radioactive substance Americum-241 (^{241}Am), which can be found in disposed smoke detectors, and which emits α-particles.

To perform the measurements, a SMPS system was used without and with different chargers to test the performance of the α-charger whereas the Ni-charger and Kr-charger is used for validation of the α-charger. Four different configurations were tried with varying number of Am-sources (3, 7, 9, and 15).

The measurements showed no consistent and reproducible behaviour of aerosol charging with the α-charger. The conclusions of this thesis is that there is a need of more controlled measurements with nebulized aerosol particles and with a different setup keeping track of the charging state of aerosol particles as described in the discussion section.

Keywords: SMPS, aerosol particles, climate change, particle number size distribution.

Acknowledgements

Firstly, I want to give the biggest thanks to my supervisors Arash Gharibi and Adam Kristensson. I am very happy that I had you by my side and that you pushed me in hard times. Arash, you made it so fun to spend time in the laboratory and you pushed me to never give up, even if the machines did not acted the way I wanted to. Adam, you are truly the master of writing scientific reports and you help me to evolve.

Further I would like to give a big thanks to Axel Eriksson and Jonas Björklund Svensson for helping me with the laboratory work. Lastly, a great thank you to Jacob Löndahl and Birgitta Svenningsson for participating in discussions and presenting great ideas for future studies.

I would like to give a big thanks to the persons who made it possible for this thesis to continue after a rocky start: Maud, Lars, Petra, Jonas, Bertil, Christian, Ing-Britt, Åsa, Tori and Hans-Olof. If you did not hand me the smoke detectors, I would not be able to finish. Even if I never met and probably will meet all of you in person, I want you to know that all of you made this thesis possible.

I would also like to say thank you to my friends for the never-ending support. All of you knew that I needed a tiny push sometimes, and you truly gave it. I am so grateful for having you as friends. Further, the greatest thanks to my family; Michael, Pia, Max and Sandra. I could not have asked for a better family, and seeing the pride in your eyes is more than enough.

Lastly, my other half. Your love, support and encouragement meant the world to me and took me to the finish line. These written words are not enough to express my gratitude for you.

List of abbreviations

AIM	Aerosol Instrument Manager
CCN	Cloud condensation nuclei
CPC	Condensation particle counters
DMA	Differential mobility analyser
DME	Diesel motor emissions
DMPS	Differential mobility particle sizer
DPE	Diesel particular matter
PSL	Polystyrene latex
RH	Relative humidity
SMPS	Scanning mobility particle sizer
HV	High voltage

List of equations		
#	**Name**	**Reference**
1	Relative humidity	Dalirian (2018)
2	The relation between mobility, dp, dimension of DMA, sheet airflow and HV-rod.	Zhou (2001)
3	Mobility transfer at the end of the DMA	Zhou (2001)
List of tables		
1	Charge distribution with a bipolar charger	Wiedensohler (1988) (Permission of use by mail)
2	Experimental sequence	Made by writer
List of figures		
1	Size range of aerosols in the atmosphere	Tomasi & Lupi (2016) (Permission of use by mail)
2	Particle chart	Made by author
3	Wave-breaking	Wilson et al. (2015) (Permission of use by mail)
4	Aeolian transport	Kok et al. (2012) (Permission of use by mail)
5	New Particle Formation	Kulmala et al. (2013) (Permission of use by mail)
6	Condensation and Evaporation	Made by author
7	Coagulation	Made by author
8	Cloud activation	Made by author
9	Brownian Diffusion	Kristensson, 2018 (Permission of use by personal communication)
10	Dry deposition	Lagzi et al. (2013) (Permission of use by mail)
11	The aerosol distribution with an optimal bipolar charger	Made by author

12	The exterior of the different chargers	Made by author
13	The interior of the α-charger	Made by author
14	The dimensions of the chargers	Made by author
15	Airflow in the α-charger	Made by author
16	Ideal transfer function of a DMA	Zhou (2001) (Permission of use by mail)
17	Differential Mobility Sizer	Institute of Atmospheric and Climate Science, (W.Y) (Permission of use by mail)
18	Condensation particle counter	The university of Manchester (2017) (Permission of use by mail)
19	3 Am-sources	Made by author
20	7 Am-sources	Made by author
21	9 Am-sources	Made by author
22	15 Am-sources	Made by author
23	Interior of the Ni-charger and Kr-charger	Made by author
24	Suggestion 1 for future studies	Made by author
25	Realistic view of a nebulizer	Made by author
26	Hypothetical view of a nebulizer	Made by author
27	Suggestion 2 for future studies	Made by author
28	Suggestion 3 for future studies	Buckley et al. (2008) (Permission of use by mail)

Table of content

Introduction

Aerosol particles affect the radiative forcing of the earth in fundamental ways. The aerosol forcing has two components, direct and indirect effects. Direct effects of aerosols are the influence on the Earth's radiation balance due to an enhancement of the natural scattering and absorption of solar radiation with an increasing concentration of aerosol particles, which result in the cooling of the Earth's surface. The indirect effect of aerosols includes their influence on cloud droplet formation. An increased aerosol concentration leads to more numerous, but smaller cloud droplets, leading to cooling with enhanced solar light scattering by the clouds. The hydrological circle of the clouds also changes, for example cloud lifetime and precipitation patterns. Further, aerosols also have an impact on human health and according to World Health Organisation (WHO), 3 million deaths every year is due to outdoor air pollution and 4.3 million deaths due to household exposure (WHO, 2017). This results in over 7 million deaths due to air pollution every year. WHO also estimates that 92 % of the world's population lives in places where air quality exceeds WHO guideline for limit values (ibid).

One of the most useful instruments to measure and assess the impact on human health and climate change of particles is the Scanning Mobility Particle Sizer (SMPS), which measures the size-dependent number concentration of particles. The instrument separates particles according to the electrical mobility in an electric field, why it requires charging of the particles

before these pass through the electric field. Commercial actors provide SMPS instruments with either a costly non-radioactive charger, or a charger containing the radioactive substances ^{85}Kr and ^{63}Ni, which are emitting ionizing β-radiation. The radiation ionizes molecules in the air, which can attach to aerosol particles making them charged with a known charge distribution. Americium-241 emits α-radiation, which also acts to ionize the air molecules. It could therefore possibly be used as a radioactive source in chargers for SMPS systems.

Aim

The aim of this thesis is to investigate the possibility to exchange the radioactive substance that is found in conventional SMPS chargers with the radioactive substance Americium-241. Can this radioactive source with the alpha particle radiation decay product give a known charge distribution of aerosol particles and be used as an alternative to the common β-radiation chargers?

Scientific questions

- How well do the measurements with SMPS containing conventional radioactive chargers correlate with the measurements made with the charger containing the radioactive substance Americium-241?
- How much charging by Americium-241 is needed to achieve a stable charge distribution of aerosol particles?

Theory

Earth’s atmosphere is a mixture of gases that surrounds the whole planet. The atmosphere makes it possible for breathing, provides protection against UV-lighting from the sun and warms the Earth up to a comfortable temperature. Further, the atmosphere is divided into four layers; the thermosphere, the mesosphere, the stratosphere and the troposphere. The layer closest to the Earth is the troposphere and it contains half of the whole atmospheric gases and most of the solid and liquid aerosol particles.

The aerosol particles differ in size, shape, composition, and mass. In the atmosphere, aerosol particles serve as condensation nuclei, and thereby act as surfaces for water vapour and other volatile gases to condense on (Colbeck & Lazardis, 2014). The effect of aerosol particle on Earth's radiation balance is significant, but there is still much concern about how much they actually cool the Earth. Aerosol particles have the ability to either directly interact with the radiation from the sun, or interact in cloud droplet formation, and thereby have the ability to create clouds that further interact with the radiation from the sun. How the radiative properties depend on particle size is shown in Figure 1, and which are the size ranges of different aerosol particle source types. The widely spread particle size range manifests the need for different measuring techniques. The particle concentration and properties can be characterized through the aerosol particle number, surface, volume or mass size distribution. Size distribution is often used as a tool to

indirectly infer climate and health effects of the particles (Friedlander, 1977).

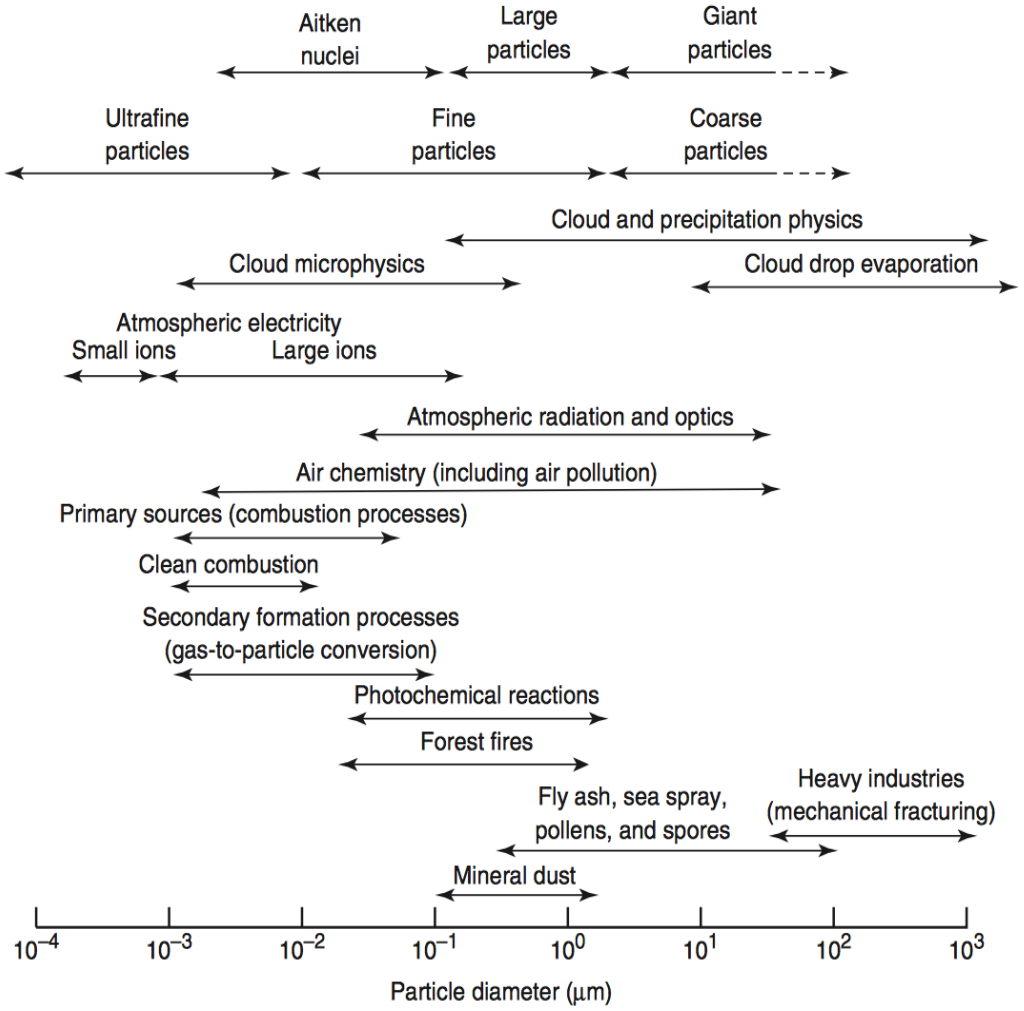

Figure 1. The size range of aerosol particles in the atmosphere and their role in atmospheric chemistry and physics (Tomasi & Lupi, 2017). Permission of use by email.

Aerosol particle sources

Aerosols take part in numerous different processes in the atmosphere, which all affect both climate change and human health. Aerosols can be both natural and anthropogenic, but only anthropogenic affect climate change. The aerosol particle sources are either primary or secondary. Primary particles refer to when particles are released to the atmosphere directly by wind, combustion or human activity (Gelencsér & Varga, 2005). Secondary particles are created in the atmosphere through gas-to-particle conversion, minutes, hours or days after the gaseous emissions (Clemet & Ford, 1999). Further, primary and secondary particles are divided into sub-groups where primary particles can originate from 3 different sub-groups: biological, emitted during combustion, or mechanically generated, while secondary particles can originate from so-called "new particle formation" and secondary formation through condensation of pre-existing particles. Figure 2 presents to some extent different sub-group of particles. Also shown are examples of sources for each of the sub-groups.

Important biological particles are fungal spores, bacteria, pollen, viruses, algae and biological crusts. There are multiple combustion sources, e.g. vehicle engine combustion, forest fires, coal power plant combustion, domestic biomass combustion, and volcanoes. Furthermore, there are four important ways in which particles are mechanically generated: wave-breaking over the sea, windblown soil dust, abrasion of the road surface from car tires and wheel brakes, and through material grinding.

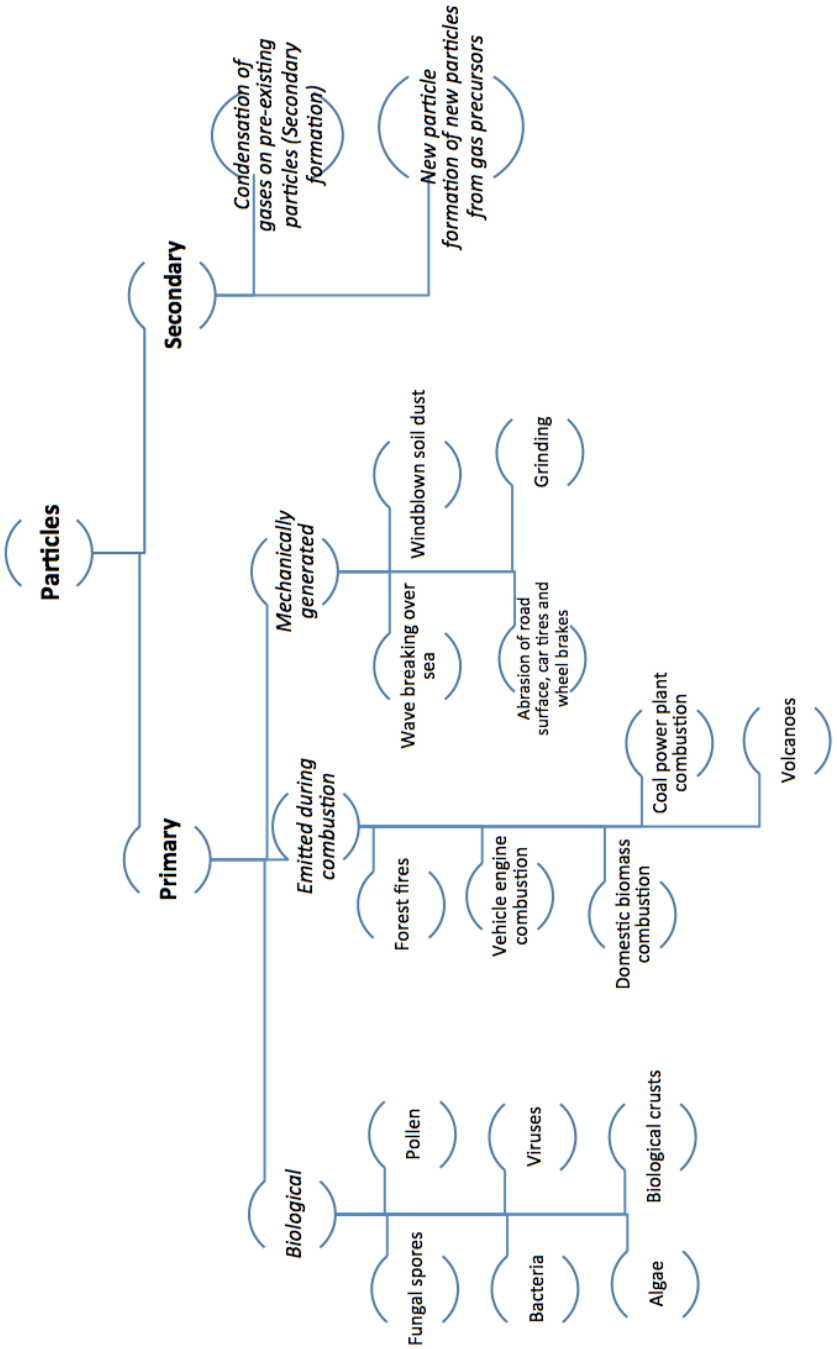

Figure 2. Primary and secondary particles and examples of sub-groups of particle sources. The figure was made by the author of this thesis (2018).

Biological particles

Biological particles (also known as bioaerosols) are airborne particles of biological origin such as viruses, bacteria, fungi and pollen (Jin Ma & Yamamoto, 2015). Bioaerosols have an important role within the interactions between the atmosphere, biosphere, human health and climate. Although the bioaerosols are vital for the reproduction of fungus, pollen, bacteria and viruses, they can cause or enhance human, animal or plant diseases (Fröhlich-Nowoisky et al., 2016).

Bioaerosols can also affect the Earth's climate system. The aerosols have the possibility to serve as nuclei, which means that they can be the seed of cloud droplets and ice crystals (Jones & Harrison, 2014). According to Hill et al. (2014), ice nucleation occurs either by freezing of the water condensed around the particle or by a particle connecting to a supercooled droplet. The ice nuclei formation depends on temperature. While other types of aerosol particles require relatively low temperatures for different freezing processes, bioaerosols dominate atmospheric ice nucleation at relative modest temperatures, above -15°C (ibid). This means that bioaerosols have the ability to greatly affect both the Earth's climate system and the hydrological cycle (Fröhlich-Nowoisky et al., 2016).

Mechanically generated

There are multiple mechanically generated particles. The four examples given in Figure 2 are described in this chapter.

Wave-breaking

The ocean represents a global source of atmospheric aerosols. According to Wilson et al. (2015) and Wang et al. (2017), aerosol sea spray particles are formed in white-caps during wave-breaking. When gas bubbles are emerging towards the sea surface, the bubbles break and produce small film drops from the breaking water bubble cap. In addition to this, larger jet drops are produced as the remnants of the gas bubble cavity collapses. The water on a fraction of the droplets will evaporate and become aerosol particles but another fraction of the droplets will not dry fast enough and will fall back in the sea due to gravity. The wave-breaking process is presented in Figure 3.

The aerosol particles contain the material that can be found in the top layer of the ocean surface. The layer contains organic material and sea salt, and the aerosol particles will contain the same compounds. However, jet drops will contain a relatively higher volume fraction of sea salt and be of a larger size, while film drops will contain a relatively higher volume fraction of organic material and be of smaller size (Wilson et al., 2015, and depicted in Figure 3).

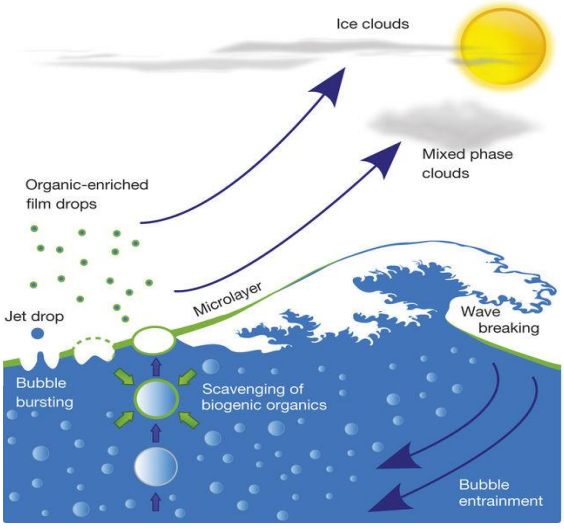

Figure 3. A sea-spray aerosol particle is generated when bubbles burst at the interface between air and sea. The film drops are enriched with organic material from the surface of the sea (Wilson et al., 2015). Permission of use by email.

Wind-blown dust

Mineral dust particles are soil particles suspended to the atmosphere in regions with dry soils, little vegetation and strong winds (Mahowald et al., 2014. Dust particles have the possibility to interact with liquid or ice clouds and thereby modify the properties and lifetime of these (DeMott et al., 2003). Dust particles can adsorb water, which creates a surface film of water. Furthermore, this can promote the formation of cloud droplets (Sorjamaa & Laaksonen, 2007) and thereby affect climate change.

When the wind is acting on a surface layer, the first particles, which will be lifted, have a diameter around 100 μm. Since they are too heavy to lift, they hop along the surface and start a process known as saltation, which start the movement of particles in other sizes making it possible for them to suspend to the atmosphere, which is depicted in Figure 4. With decreasing dust particle size, there is an increasing lifetime and travel distance of dust particles (Kok et al., 2012; Karydis et al., 2017).

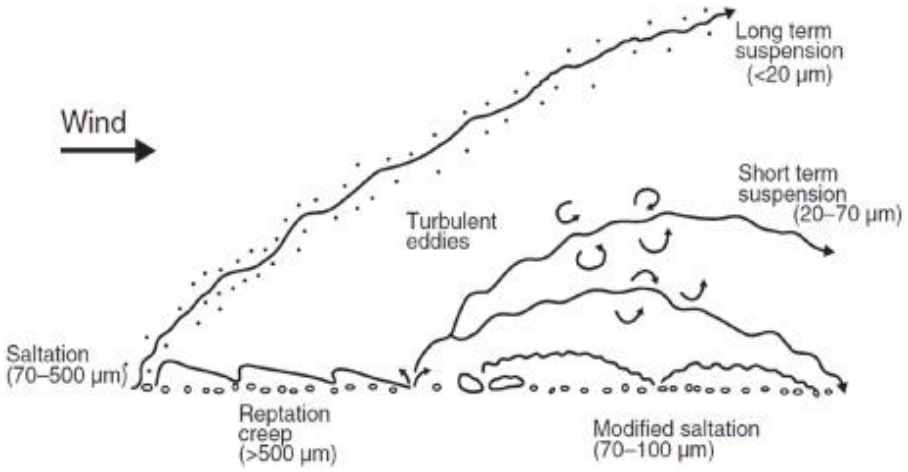

Figure 4. Modes of aeolian transport (Kok et al., 2012). Permission of use by email.

Abrasion of road surface, car tires, and wheel brakes

Particles from roads, pavements and tires contribute to higher concentrations of inhalable particles in outdoor air. This occurs to a larger extent during dry periods in winter and spring because of the use of studded tires and gritting. As the road surfaces dry up, a large amount of grinded material becomes airborne and creates large mass concentrations of PM_{10}[1] (Gustafsson et al., 2009; Fullova & Durcanska, 2016). As vehicles are moving on the surface, the contact between the wheels and the surface leads to grinding at the contact angle of both surface and wheel material. In addition, the actual breaking of the vehicle leads to degeneration as the brake block acts on the disc brake. All of this leads to emissions in the atmosphere of particles, which are called vehicle abrasion particles.

The asphalt particles contain directly emitted sharp-edged mineral and bitumen[2] particles, which could be of special interest for health-mediated effects (Bhardawaj et al., 2017).

Grinding

Grinding produces many different types of particles depending on what kind of material is being grinded. One type of grinding is construction activity, for example sawing in concrete, where several processes of grinding are happening and thereby creating a high concentration of particles within the area (Bradshaw, 1951).

---

[1] Particles of 10 μm in diameter or less (Querol et al., 2004).

[2] The generic term for a semisolid mixture of hydrocarbons mostly used in asphalt (Salou et al., 1998).

Emitted during combustion

Particles can be produced and thereby emitted during different combustion processes. Two of the most common processes types are presented below.

Diesel exhaust

Diesel motor emissions (DME) have an important role regarding the discussions about human health and human exposure to particles in their daily life. DME contains a mixture of hundreds of components in either gas or particulate form, e.g. carbon monoxide, sulphur compounds, nitrogen compounds and several low-molecular-weight hydrocarbons. Diesel particulate matter (DPE) contributes to fine particles ($PM_{2.5}$[3]) mass concentrations, and have a high fraction of ultrafine particles (<0.1 μm). Their small size makes them easy to inhale and travel far in the respiration system of humans such as deep in the lung and even in the blood circulation system (Wichmann, 2007).

Cars and other heavy-duty and light-duty vehicles are the most important sources of DME. However, non-road diesel engines in locomotives, marine vessels, etc. also have an important role in human exposure to particles. Between these types of sources, DME varies both in chemical composition and particle size among different types of engines, the way the engine is being operated and fuel composition.

[3] Particles of 2.5 μm in diameter or less (Zhang et al., 2013).

Biomass combustion

Forest fires, domestic wood combustion, and biomass combustion in large energy plant facilities are the three most important biomass combustion sources of particles. The three sources result in particles with similar, but not equal chemical composition. In comparison with diesel combustion, ash particles are more often found in biomass combustion, and depending on the burning conditions, soot particles are also less common in biomass combustion (Johansson et al., 2003).

Secondary particles

This chapter will present two different processes of secondary particles: new particle formation and secondary formation through condensation.

New particle formation

New particle formation, also called nucleation, refers to the production of new particles, charged or neutral, which are between 1 and 2 nm in diameter when formed. New particle formation via nucleation is an important source of particles and may have an influence on climate by altering the distribution (Pettibone, 2009). There are several theories behind new particle formation. One of them called cluster activation theory, involves a three step process. The first step includes cluster formation by gas-phase reactions. The second step is the homogeneous or ion-induced nucleation of either neutral or ion clusters. The last step involves the growth of these clusters into larger particles. The processes are presented in Figure 5, which also shows at which diameters the different process is taking place (Kulmala et al., 2013).

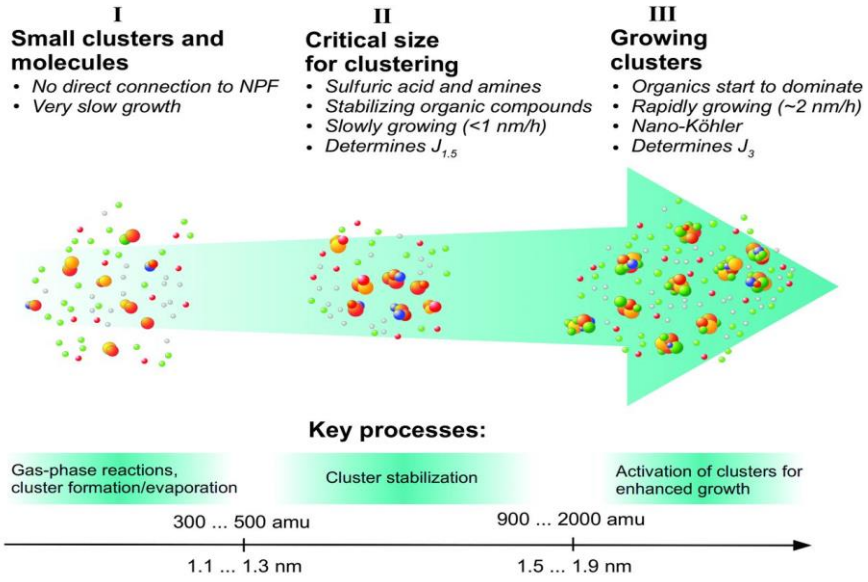

Figure 5. The different steps that a new particle formation contains of and key processes that every step has. (Kulmala et al., 2013). Permission of use by email.

Secondary formation

There is an increased particle mass concentration in the atmosphere through condensation of gaseous compounds on pre-existing particles. Sulphur dioxide, nitrate, ammonia, and organic compounds of lower volatility are examples of chemical species condensing on particles, making their mass larger (Verheggen & Weijers, 2010). The actual process of condensation is, however described in the next section.

Particle processes

Particles can participate in several different processes when emitted in the atmosphere, which has fundamental effects on the chemical composition, size, and lifetime of aerosol particles during long-range transport in the atmosphere. The mane processes of condensation/evaporation, coagulation and cloud activation will be described in this chapter.

Condensation/evaporation

Condensation is when gases adhere to existing atmospheric particles in the atmosphere and thereby make the atmospheric particles larger with an increasing mass concentration without changing the number concentration. The reverse process is called evaporation, where the aerosol particle is shrinking since gas is evaporating from the aerosol particle (Wagner, 1982).

When a gas molecule is condensed to an existing particle, it can either stick to the surface of it, or it can dissolve in the liquid interior of liquid aerosol particles. This can result in changed chemical properties due to the chemical reactions that occur in the liquid phase. Figure 6 shows a simplified picture of these processes.

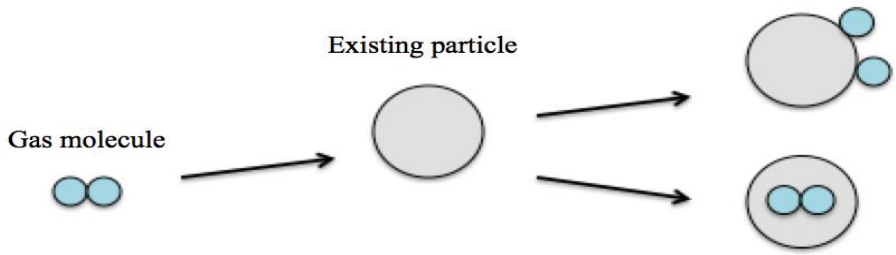

Figure 6. A schematic description of the processes condensation and evaporation, which includes aerosols. The figure was made by the author of this thesis (2018).

Coagulation

When two particles collide and adhere to each other, it will reduce the number concentration in the atmosphere of aerosol particles, but leave the mass concentration unchanged. At the same time, the new coagulated particle is larger than the two original ones. Figure 7 presents the alternatives for the particles; either they can dissolve into each other or form agglomerates. Further, if one of them is solid, a solid core can be formed in the center of the new particle (Jacobson & Turco, 1995).

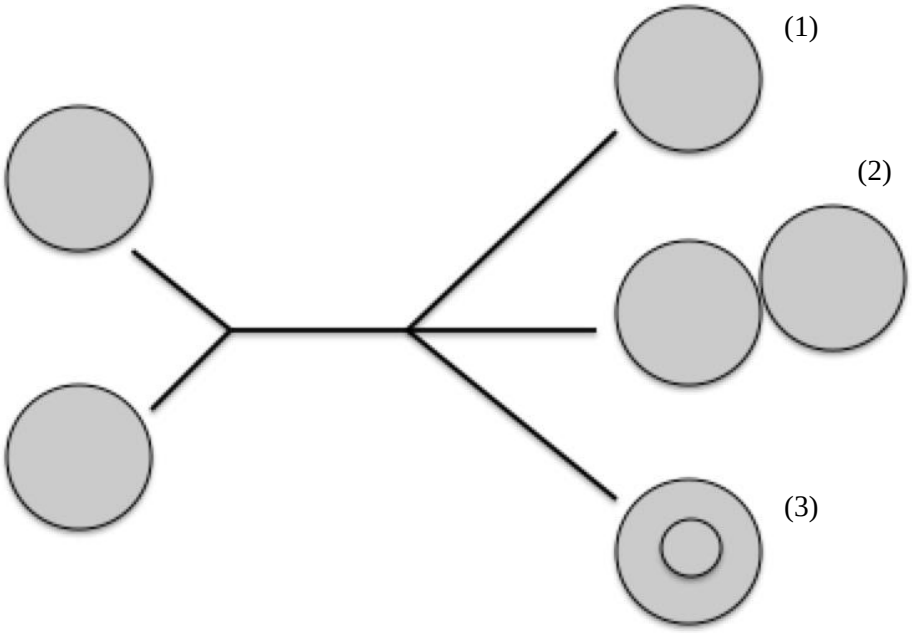

Figure 7. Coagulation options for atmospheric particles where (1) is when two particles have dissolved into each other, (2) are agglomerates and (3) is a new-formed particle with a solid core. The figure was made by the author of this thesis (2018).

Cloud activation

The hygroscopic growth of aerosol particles by the uptake of water is called water vapour condensation, which depends on the atmospheric relative humidity (RH). RH expressed in % is defined as by (1) Dalirian (2018):

$$RH = \frac{P_w}{P_w^\circ} \, x \, 100 \qquad (1)$$

P_w = Partial pressure of water vapour at a given temperature

P°_w = Saturation pressure of water vapour at the same temperature

Figure 8 presents the necessary steps for cloud activation to take place. Lohmann et al. (2016) and McFiggans et al. (2006) argue that the first step of activation is the hygroscopic growth, which refers to subsaturated conditions where the RH is below 100 %. As the air becomes supersaturated[4] with humidity high enough for the particles to reach a critical size threshold, the cloud condensation nuclei (CCN) particles can activate and form cloud droplets (Lohmann et al., 2016).

[4] Supersaturnation is the state of a solution that contains more of the dissolved material than what could be dissolved by the solvent under normal circumstances (Kulkarni et al., 2011).

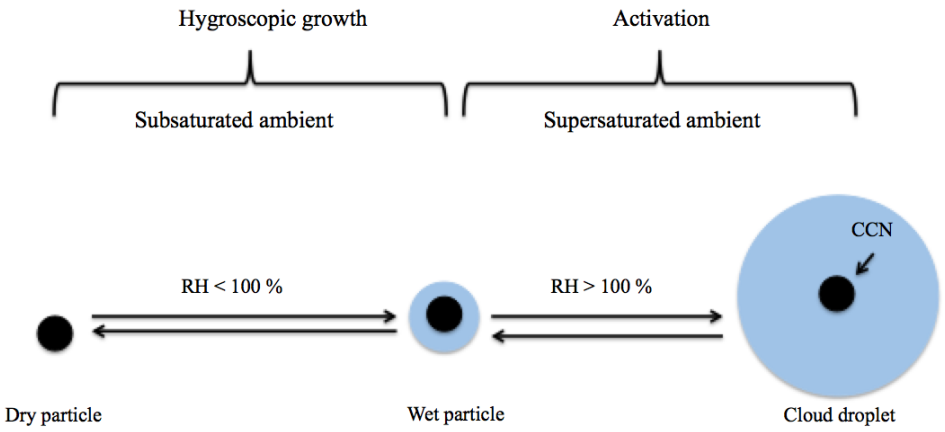

Figure 8. Representation of aerosol particles growth and activation by condensation of water vapour. The figure is made by the author of this thesis (2018).

Dry and wet deposition

Deposition of air pollutants is an important loss of gases and aerosol particles from the atmosphere. There are two types of deposition, wet and dry depositions. The dominant loss process of aerosol particles is wet deposition, which accounts for the removal of 80-85% of aerosol particles. In areas with high yearly precipitation, wet deposition dominates, but in areas where precipitation is not common, dry deposition takes over (Connan et al., 2012).

Wet deposition

There are two types of wet deposition: *In-cloud scavenging* and *below cloud scavenging*. In-cloud scavenging occurs inside of clouds after CCN

activation and subsequent rain droplet formation (Boucher, 2015). Below cloud scavenging occurs under the clouds due to falling rain droplets that collide with aerosol particles by Brownian diffusion, interception and impaction, which is described in Figure 9. The Brownian diffusion means that nano-sized particles are deviating from the air streamlines around the droplets and thereby may impinge on the water surface. Further, interception works in the way that a larger sized aerosol particle passes along air streamlines. If the particle is too close to the water surface, it will also impinge on the droplet. Impaction also works with larger particles, and is the processes in which particles are forced to deviate from an airstream and thereby hit or impact the droplet due to their inertia. The chance of collision increases with the size of the aerosol particles (Seinfeld et al., 2006).

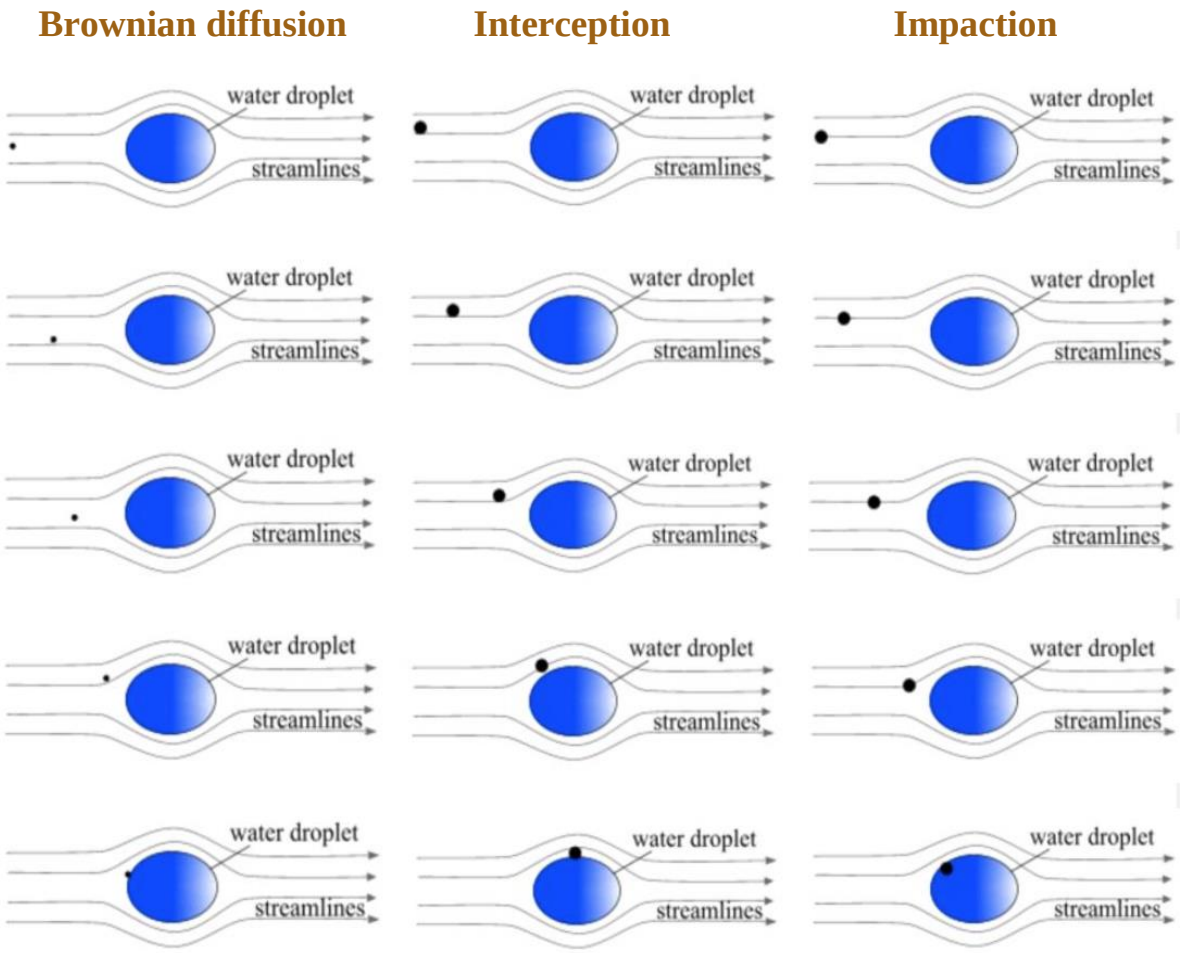

Figure 9. Description of Brownian diffusion, interception and impaction between an aerosol particle (black dot), and a rain droplet (blue sphere) (Kristensson, 2018). Permission of use by personal communication.

Dry deposition

Dry deposition depend on the properties of the gases or particles and the removal process is strongly depending on several environmental factors, i.e. Brownian diffusion[5], impaction, interception, electrostatic attraction, weather conditions, near-surface conditions and particle properties (Mohan, 2015; Lagzi et al., 2013). According to Ruijgrok et al. (1995), dry deposition mainly occurs when the particles are relatively close to the surface area, which can consist of multiple types of surfaces, for example vegetation, water and human constructions.

The prime mechanism for dry deposition is likely turbulent diffusion (Mohan, 2015; Hemond et al., 2015, Figure 10) since it has a large contribution to the Brownian diffusion over the ground surface (Zhang et al., 2014). Turbulent diffusion is defined as the transport of mass, heat or momentum within a system due to random and chaotic time dependent wind movements (Shimada et al., 2006; Ounis et al., 1991).

[5] Brownian diffusion is the chaotic and irregular movement of a particle caused by its collisions with the surrounding molecules of much smaller size (Batchelor, 1976).

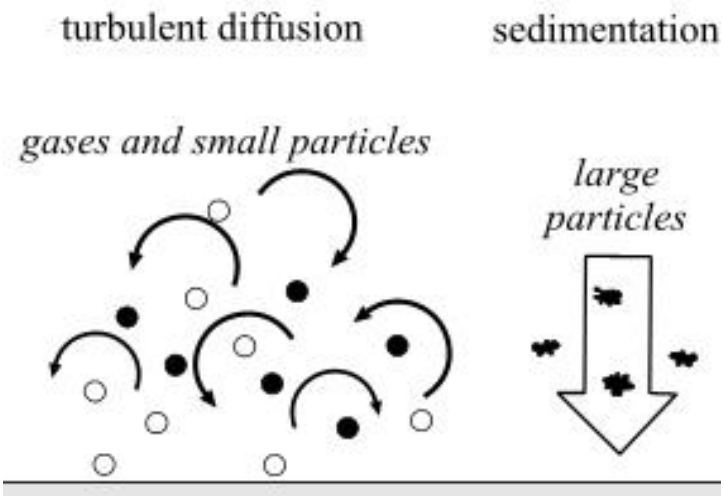

Figure 10. The dry deposition of smaller and larger sized particles, respectively (Lagzi et al., 2013). Permission of use by email.

Atmospheric charges

Electrons and ions are present in the atmosphere, where negative ions are more numerous at low altitudes due to the attachment of electrons to oxygen molecules. With increasing altitude, the atmospheric density decreases and the ability of an electron to attach to an oxygen molecule decreases. The presence of solar radiation leads to destruction of negative ions and positive ions take over (Smirnov, 2017). In addition to single negative and positive ions in the atmosphere, ions can also have multiple negative and positive charges i.e. -3, -2, +2, +3 etc.

One process that occurs continuously in the atmosphere is ionization through cosmic radiation. Over the land areas, additional ionization is caused by alpha-radiation from radon decay and gamma rays emitted from soil and

rock. Further, there is also minor local ionization occurring that contributes to the total ionization of the atmosphere, for example from power lines (Eisele, 1989), but their contribution is small (Leppä, 2012).

There are many methods that contain different techniques and devices to enable measurements of particle charges. Hochrainer (1985) and Brown (1997) classified the different methods in two categories: 1) static or direct and 2) dynamic. The static or direct methods measure the absolute charge, and the dynamic methods measures electrical mobility and extract charge information (Buckley et al., 2008). Flagan (1988) presents an historical review of the techniques and methods of measuring charged particles, and also presents the common denominator; electrical mobility (mobility data).

When mobility data is measured, it can be converted into a size distribution if the charge distribution is known to some extent. According to Beckley et al. (2008), this is achieved by bringing the aerosol into charge equilibrium with the ionic atmosphere in a bipolar diffusion charger, also known as neutralizer. Then, the fraction of charged particles of a given size can be calculated with existing bipolar charging theories from i.e. Fuchs (1963) and Wiedensohler (1988). This is the kind of charger used with SMPS systems to measure the particle number size distribution.

Fuchs (1963) describes the limiting sphere of bipolar diffusion charging of aerosol particles. For an aerosol the fraction of particles carrying up to two charges is calculated using the theory Fuchs (1963) is presenting in the article together with the ion mobility ratio (Wiedensohler, 1988), ion masses from Hussein et al. (1983) and the probability of collision of ions with the particle (Hoppel & Frink, 1986). For particles with 3 or more charges, the analytical solution presented by Gunn (1955) is used (Beckley et al., 2008).

Wiedensohler (1988) presents the percentage distribution of bipolar diffusion charging of aerosol particles (Table 1). Further, Figure 11 presents how the aerosol charge distribution will look like after charging with a bipolar charger.

Table 1. Charge distribution with a bipolar charger (Wiedensohler, 1988)
Percentage of aerosol that attain a specific charge when passing through a bipolar charger. f (N) is the percentage of aerosols and D_p is the diameter of the aerosols presented in nm. Permission of use by email.

***f* (*N*) (%)**					
D_p	**-2**	**-1**	**0**	**+1**	**+2**
1	0	0,47	99,09	0,44	0
1,3	0	0,58	98,88	0,54	0
2	0	0,85	98,38	0,77	0
3	0	1,27	97,62	1,11	0
5	0	2,21	95,92	1,86	0
7	0	3,28	94,03	2,69	0
10	0	5,03	90,96	4,02	0
13	0	6,87	87,73	5,40	0
20	0,02	11,14	80,29	8,54	0,01
30	0,17	16,35	71,03	12,35	0,10
50	1,13	22,94	58,10	17,20	0,63
70	2,80	26,02	49,99	19,53	1,57
100	5,67	27,42	42,36	20,75	3,24
130	8,21	27,30	37,32	20,85	4,77
200	12,18	25,54	29,96	19,65	7,21
300	14,56	22,71	24,16	17,51	8,65
500	15,09	18,60	18,28	14,33	8,95
700	14,29	15,94	15,15	12,27	8,46
1000	12,86	13,33	12,36	10,24	7,59

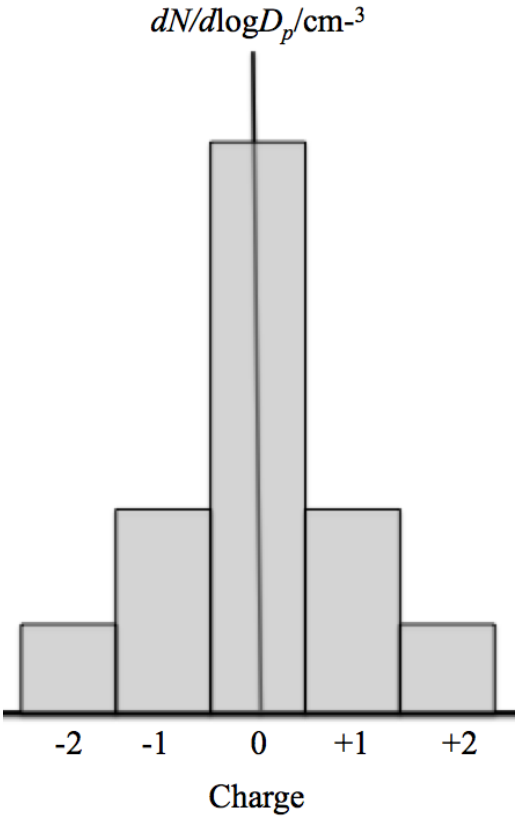

Figure 11. The schematic distribution of charged aerosol particles of a given type. Fundamentals presented in Wiedensohler (1988) with permission of use by email.

Ionization of alpha-particles

Robert Millikan performed floating oil drop experiments, where he charged the oil drops with different charges in different experiments. In one of his experiments, alpha radiation sources were used as the radioactive source. In air, gas molecules are bombarded by alpha particles. From each impact, an electron is emitted from one of the outer shells, creating a positive ion in the

air. This process is repeated multiple times until the alpha particle has lost its kinetic energy. The produced electrons attach to other gas molecules creating negative ions. Robert Millikan discovered that most oil drops contained only a single charge after ionization with α-particles, and very few double charges (Millikan et al., 1920). The oil drops can potentially be compared to aerosol particles. Hence, these experiments showed that α-decay was not promising in order to attain a charge distribution similar to Table 1. However, the oil drop experiments do not compare exactly to atmospheric particles and conditions, why it is worth testing regardless of the outcomes of the Millikan experiments. Even if the charging state looks differently than in Table 1, maybe it is anyhow reproducible and can be used for SMPS systems.

The chargers

In this thesis, 3 different types of bipolar chargers were used; Kr-charger, Ni-charger and α-charger (Figure 12). The Kr-charger has a cylindrical form with an inlet and outlet in the same shape and has a half-life of 10.8 years. The Ni-charger has the same shape, contains ^{63}Ni, and has a half-life of 100 years. The α-charger differs strongly in shape, and contains ^{241}Am collected from disposable smoke detectors, which has a half-life of 432.2 years.

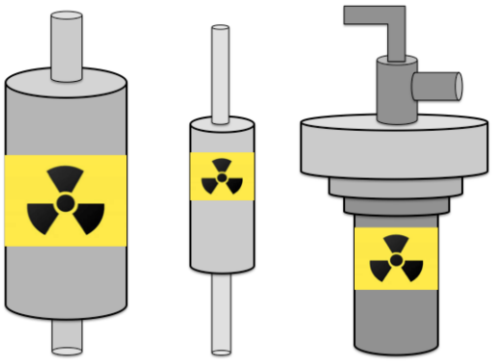

Figure 12. The exterior of the chargers. The figure was made by the author of this thesis (2018).

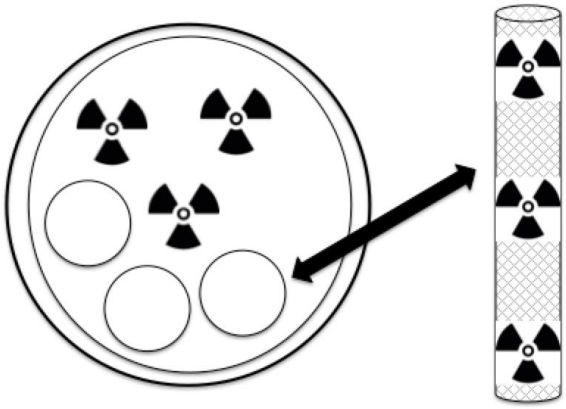

Figure 13. The interior of the α-charger and the location of the Am-sources. The figure was made by the author of this thesis (2018).

The exterior of the chargers is presented in Figure 12 and the interior of the α-charger is presented in Figure 13. There are 3 blocks of Am-sources glued to the bottom of the α-charger, and scattered around it is tubes of thin net with a maximum of 3 Am-sources in each.

The chargers have similar heights and diameter. The α-charger has a height of 18 cm, Kr-charger 16 cm and Ni-charger 15 cm. The diameter of the α-charger is approximately 6 cm, Kr-charger 5 cm and Ni-charger 3 cm. Figure 14 presents the dimension of the different chargers by a picture taken in the laboratory.

Figure 14. A presentation of the dimensions of Ni-charger, Kr-charger and α-charger. Picture was taken by the author of this thesis (2018).

Since the α-charger is different in construction compared to the Kr-charger and Ni-charger, we need to present the airflow inside the charger in Figure 15 for comparison. The airflow enters through a separate entrance and continuous further down by a narrow steel tube that has 3 small openings where the airflow can exit to the radioactive volume. The charged airflow then enters the small tube of openings again and continuous to a separate exit.

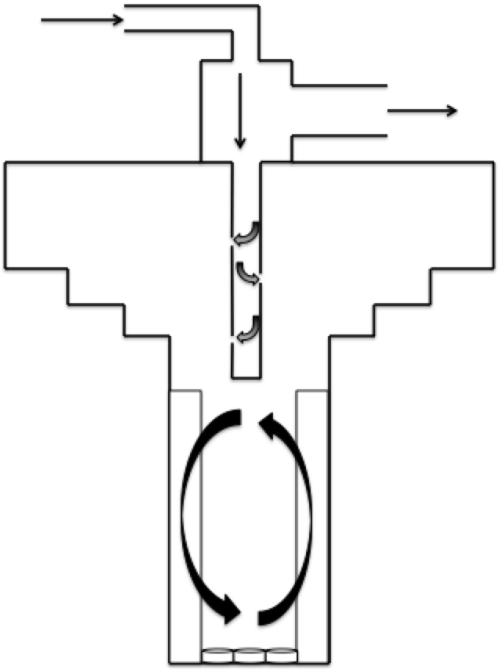

Figure 15. The figure presents how the airflow travels in the α-charger. The figure was made by the author of this thesis (2018).

Scanning mobility particle sizer (SMPS)

There are basically three components of an SMPS system; the charger, the DMA and the CPC. The air is first lead through the charger (either Kr or Ni normally), where the aerosol particles attain a known charge distribution as described above. The sample then continues to the DMA. The DMA is a cylindrical capacitor consisting of an inner electrode, also known as the high voltage rod (HV-Rod), and an outer electrode. The inner electrode has an

electric potential compared to the outer electrode, which is grounded, and therefore there is an electric field between the inner and outer electrode. When the aerosol sample enters the DMA, the flow is oriented parallel to the HV-Rod, and driven by the higher, and clean sheath airflow.

If the particles are charged, they will be deflected by the electric field, either towards the central rod if the central rod and particles have opposite charges, or towards the outer cylinder if they are not of opposite charge. The degree of deflection depends on the electric mobility of the particle. It is defined as the ratio of the constant limiting velocity a charged particle will reach in a uniform electric field to the magnitude of this field (Knutson, 1976). The electrical mobility mainly depends on the particle size and electrical charge. The smaller the particle and/or the higher the electrical charge, the higher is the electrical mobility. By regulating the voltage in the HV-rod in the DMA, different sizes of particles can be led through the aerosol out slit at the end of the DMA as depicted in Figure 14, and detected by the CPC.

The relation between the mobility, the particle diameter, dp, dimensions of the DMA, sheath air flow, and the HV-rod voltage is described by the following so called DMA formula (2) (Zhou, 2001):

$$Z_p = \frac{neC_c}{3\pi\eta D_p} = \frac{Q_{sh}\ln(\frac{r_2}{r_1})}{2\pi VL} \qquad (2)$$

where Z_p is the particle electric mobility, *n* is the number of charges, *e* the elementary charge, C_c the Cunningham slip correction, η the air viscosity, D_p is the particle diameter, Q_s is the aerosol sampling outlet flow rate, r_1 and

r_2 the inner and outer radius of the HV-rod, V is the voltage applied to the classifier and L is the axial classifier inlet and outlet slit separation.

Since the geometry and flow relations are not perfect in the DMA, there will not be a discrete particle mobility exiting the DMA. The particle number electric mobility distribution exiting the DMA in the end slit is ideally described by a triangular transfer function. It is assumed that 100 % of the particles at the mobility Z_p corresponding to the particle diameter Dp exiting the DMA, while 0 % of the particles continue to the DMA at the mobilities $Z_p+\Delta Z_p$ and $Z_p-\Delta Z_p$. The width of the mobility transfer function at the end slit of the DMA is described as (3) (ibid):

$$\Delta Z_p = 2 \times \frac{Q_a}{Q_{sh}} \times Z_p \quad (3)$$

where ΔZ_p is transfer function base half width and Q_a is the aerosol flow. Hence, by decreasing the ratio between the aerosol and sheath flow of the DMA, the mobility (and size resolution) is improved in the DMA. This is the reason why most DMA are set at low aerosol flow and high sheath flow. On the other hand, a high sheath flow does not allow the sampling of very large particles according to the inverse relationship between these two parameters in the DMA formula. Hence, choosing relatively small sheath air flows and thereby lower size resolution of the DMA is a necessity when sampling larger particles. A simplified transfer function of a DMA is presented in Figure 16.

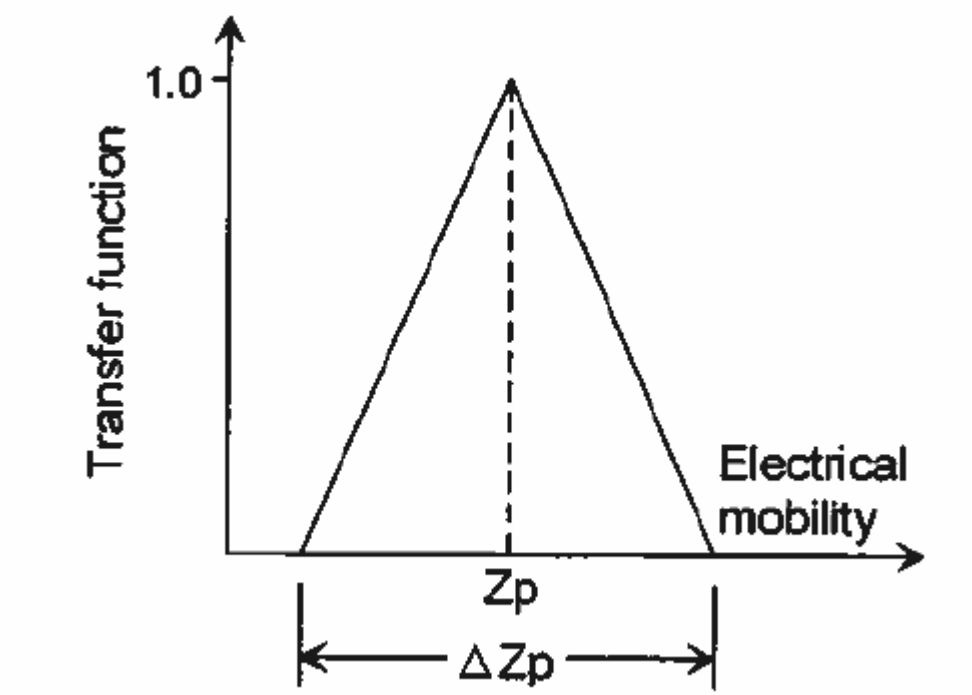

Figure 16. Simplified and ideal transfer function of a DMA (Zhou, 2001). Permission of use by email.

When counting the particles exiting the DMA (Figure 17) with a CPC, a particle number size distribution can be estimated by applying different voltages on the DMA and by using the DMA formula in combination with the transfer function of the DMA.

In reality, the width of the transfer function is increased due to broadening of particle trajectories inside the DMA, and the area of the transfer function is lowered due to particle diffusional losses in the DMA. This needs to be taken into account when calculating the final particle number size distribution (Zhou, 2001).

Ideally, we only sample particles with a single charge and well-defined electric mobility. However, since there are also doubly and triply charged

particles of a higher diameter, but with the same electrical mobility leaving the DMA exit slit, there is a need to subtract for the concentration of these large particles when estimating the final particle number size distribution. The collection efficiency of the CPC as function of particle diameter also needs to be taken into account, and the transport time between the DMA and the CPC, and the different residence time of particles inside the relatively large volume of the CPC. In an SMPS system (as opposed to a DMPS system, Differential Mobility Particle Sizer), the voltage is scanned continuously up or down in the DMA. In other words, the particle trajectory inside the DMA is rather complicated as the voltage is changing. This also needs to be taken into account when calculating the final particle number size distribution. Since, some of the confounding factors are dependent on the other factors at the same time, this correction should not be performed individually for the different factors. Rather, all factors should be considered simultaneously in a single matrix inversion calculation as described by Zhou (2001).

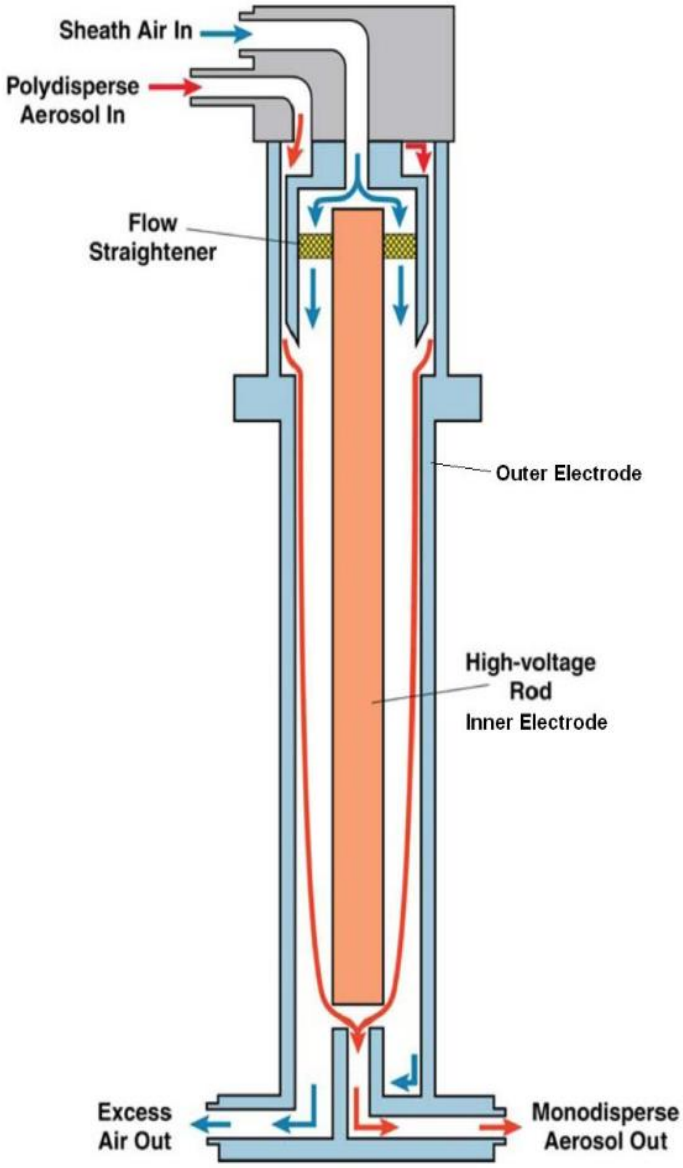

Figure 17. The function of a DMA (Institute of Atmospheric and Climate Science, W.Y). Permission of use by email.

Condensation particle counter (CPC)

A condensation particle counter (CPC) detects and counts aerosols by enlarging them. This is performed using the particles as nucleation centres to create droplets in a supersaturated gas by cooling, which is referred to as the diffusional thermal cooling method (Ahn et al., 2005).

In a counter for using the diffusional thermal cooling method, air containing particles passes through a heated porous block, which is in contact with a working fluid, usually butanol and becomes saturated. Further, the saturated air is cooled in the condenser block and thereby becomes supersaturated which causes particles above a certain size to grow into drops. These drops pass through a laser beam are counted (Figure 18). The minimum particle size, which can be detected by the CPC, depends on the supersaturation achieved, and this is depending on the temperature difference between the saturator and condenser (The University of Manchester, 2017).

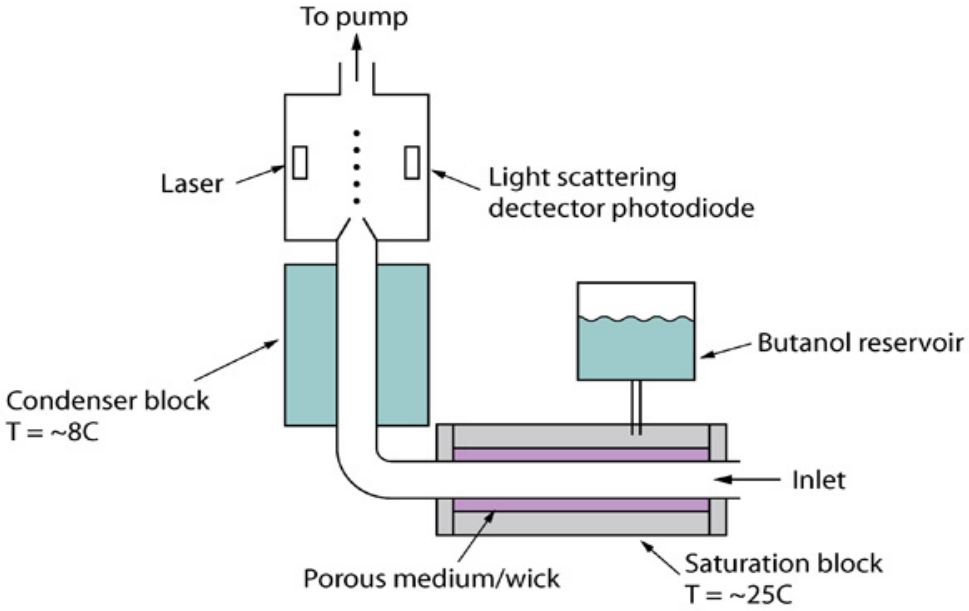

Figure 18. The schematic of a CPC that can count the aerosols due to the enlargement and laser technique (The University of Manchester, 2017). Permission of use by email.

Methodology

A TSI Scanning Mobility Particle Sizer (SMPS) model no. 3028 was used to perform the experiments where the aerosol flow is set to 1 L/min and the sheet flow is set to 8 L/min. The program used to steer the instrument and interpret the data collected was Aerosol Instrument Manager (AIM). First, the aerosol particles are charged according to a known charge distribution, normally with a krypton or nickel charger. Then, the aerosol flow enters the Differential Mobility Analyzer (DMA), where particles with a certain electrical mobility pass through the aerosol outlet of the DMA. Finally, the Condensation Particle Counter (CPC) (model 3771, TSI Inc.) counts the aerosol particles in the airflow at different aerosol sizes. Further information about the fundamentals of an SMPS system and its components is described in the theory section.

The experiments were performed with normal room air in the aerosol laboratory, at Lund University, Department of Design Sciences, Lund, Sweden. The lab air in the aerosol laboratory is similar to the outdoor urban background air present outside the aerosol laboratory, except for the fraction particles lost in the ventilation system of the house, and the particles produced inside the lab room. Nevertheless, the room air was not controlled in any way, and the concentration and shape of the collected size distribution varied substantially between different days and different hours of the day.
The measurement sequence during the experiments is shown in Table 2. First, when lab air was measured with the SMPS, no charger was connected

to the SMPS system. This part of the experiment sequence has the working name “No charger”. Since, also room air aerosol particles are charged to a certain degree due to naturally occurring ions in the atmosphere, it resulted in significant counts and reasonable particle number size distribution during the different experiments. The “No charger” measurements were performed to test how the different chargers were able to change the charge distribution and hence, the particle number size distribution to a more correct one after charging.

In the second step of the measurement sequence, the Kr-charger was used before the SMPS system. In the third sequence, the Ni-charger, and during the final fourth sequence, the α-charger was used before the SMPS.

The scanning time of the SMPS was set to 3.16 minutes (190 seconds). Due to a short time of inactivity between each measurement sequence when switching the chargers, the whole 4-step sequence took about 13 minutes. This 4-step sequence was repeated between about seven to ten times in the same day. This entire experimental procedure then took more than 2 hours to perform.

The entire experiments were procedure during 3 different days. During these different days we were able to repeat the entire experimental procedure 4 times, with 4 different numbers of Am-sources: 3, 7, 9, and 15 chargers. In the last experiment, which took longer time, we also alternated with measurements by a CPC to measure the total number concentration and how this compares to the total number concentration from the SMPS size distribution.

Table 2. Experimental sequence
The table shows in which order the different experiments with different chargers were performed. This sequence was performed between 7 and 10 times. This entire experimental procedure was repeated 5 times as explained in the text section.

#	No charger	Kr-charger	Ni-charger	α-charger
1				
2				
3				
4				
5				
6				
7				
8				
9				
10				

Results

The results from the 4 experiments are presented in the following. Each experiment consisted of between 7 and 10 repeated measurements according to a well-defined measurement sequence. In each measurement sequence, the measurements alternated between measurements with 1) no radioactive charger, 2) the Kr-charger, 3) the Ni-charger, and 4) the tested α-charger. For each of the 4 experiments, 3, 7, 9, and 15 Am-sources were used respectively, were also CPC measurements were performed during the last experiment to compare with total number concentrations as described in the methodology section.

The result presented below is the average of the particle number size distribution of the between 7 and 10 measurements for each experiment. The size distribution can vary relatively much during the course of the day, since normal room lab air is measured. For this reason, the reader has the possibility to also investigate the individual 7 to 10 measurements for each day in Attachments 1 to 4.

The average of the measurement day with 3 Am-sources is presented in Figure 18. The *x*-axis presents the particle diameter on a logarithmic size scale, and on the *y*-axis the number concentration of aerosols is presented as $dN/d\log^{10}D_p$ (cm^{-3}). In short throughout the report, we denote it as $dN/d\log D_p/cm^{-3}$.

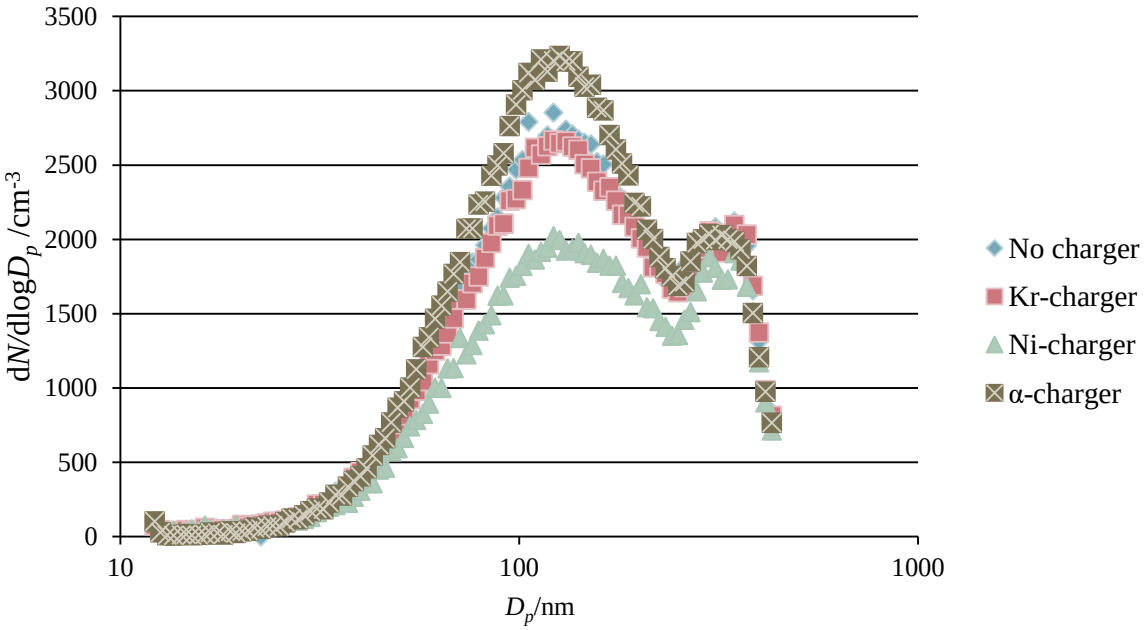

Figure 19**.** The average particle number size distribution where the α-charger contain 3 Am-sources. There are 10 measurements performed for each measurement sequence, and the average is calculated for these 10 measurements.

As we can see in the SMPS size distribution, the particle number concentration of the Kr-charger and Ni-charger are at or below the concentration with no charger. Likely, the lab room air contains particles, which have more charges than the particles after charging with the Kr-charger and the Ni-charger. Hence, it is likely that the chargers take down the number of charges of the particles compared to the lab room air particles, and this makes the particle number concentration lower when chargers are connected compare to the no charger experiment. The Ni-charger takes down the concentration to a higher extent than the Kr-charger, which might be due

to the fact that the Kr-charger is no longer effective due to the short lifetime of Kr radioactive sources (10.8 years). Since the concentration with the α-charger is higher than that with no charger, it can be indicative that the Am-sources is producing more charges on the particles than found in the lab room air.

An alternative explanation involves assuming that the room air particles have less charges attached to them than after passing through conventional chargers. In our case, the Ni-charger is possibly not effective at charging the particles, since the charger is possibly dirty, leading to a large loss of small particles through diffusion or interception without charging them properly. Since the measurements with the Kr-charger resemble those of the no charger measurements, it could mean that the charger is no longer able to change the charge distribution of room air particles to a large extent due to the short lifetime. These explanations could in theory mean that instead; the Am-sources are able to bring particles to a higher and more correct bipolar charging state than the other chargers, and is showing a more correct concentration than the other chargers. We realize that this explanation is far-fetched, and would probably require a serious problem with the Ni-charger. Cleaning the charger and compare measurements before and after the cleaning could in future test this.

There could also be other explanations for the observed tendencies, which we are not familiar with, or lack information to be able to find alternative explanations.

To continue the evaluation of the α-charger, 7 Am-sources were used during the next measurement day (Figure 20). This time, all chargers result in lower concentrations for particles smaller than 200 nm diameters than

with no charger. It could mean for example that the room air particles on this current day of measurements are extremely highly charged, and that no matter the functionality of the different chargers, they all take down the charging state of the particles and make the concentration lower.

The plausible difference of the charging state of the room air aerosol during the measurement days with 3 and 7 Am-sources shows that there is a need to control the charging state of the room air aerosol particles to be able to conclude what is happening. Alternatively, one needs to perform measurements with a different method to find out about the functionality of the α-charger as suggested in the discussion section.

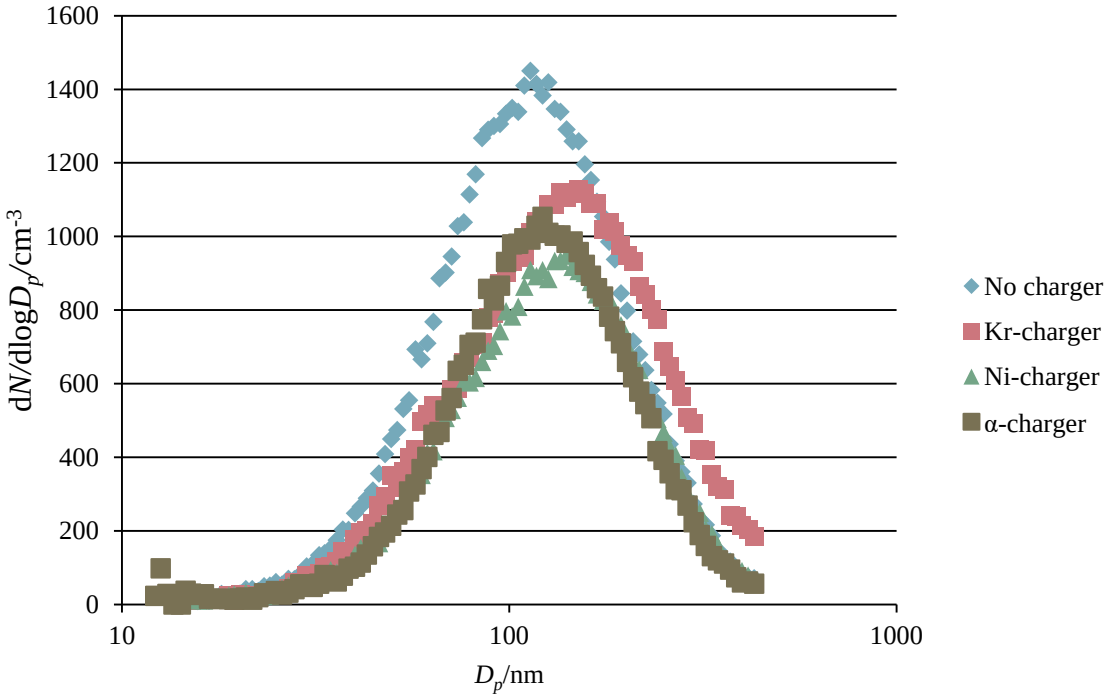

Figure 20. The average particle number size distribution where the α-charger contain 7 Am-sources. There are 10 measurements performed for each measurement sequence, and the average is calculated for these 10 measurements.

In the experiment with 9 Am-sources (Figure 21), the results were quite similar to the experiment with 7 Am-sources (Figure 20). Hence, we do not provide further alternative explanations to the situations than what we have done previously. We note that we have possibly reached saturation with the Am-sources. Having 7 or 9 Am-sources might not give large differences in the size distributions. However, we realize that statistically, we cannot conclude possible differences between the two experiments, and besides, the size distributions have different shapes between the two different experiment days, which makes the comparison difficult.

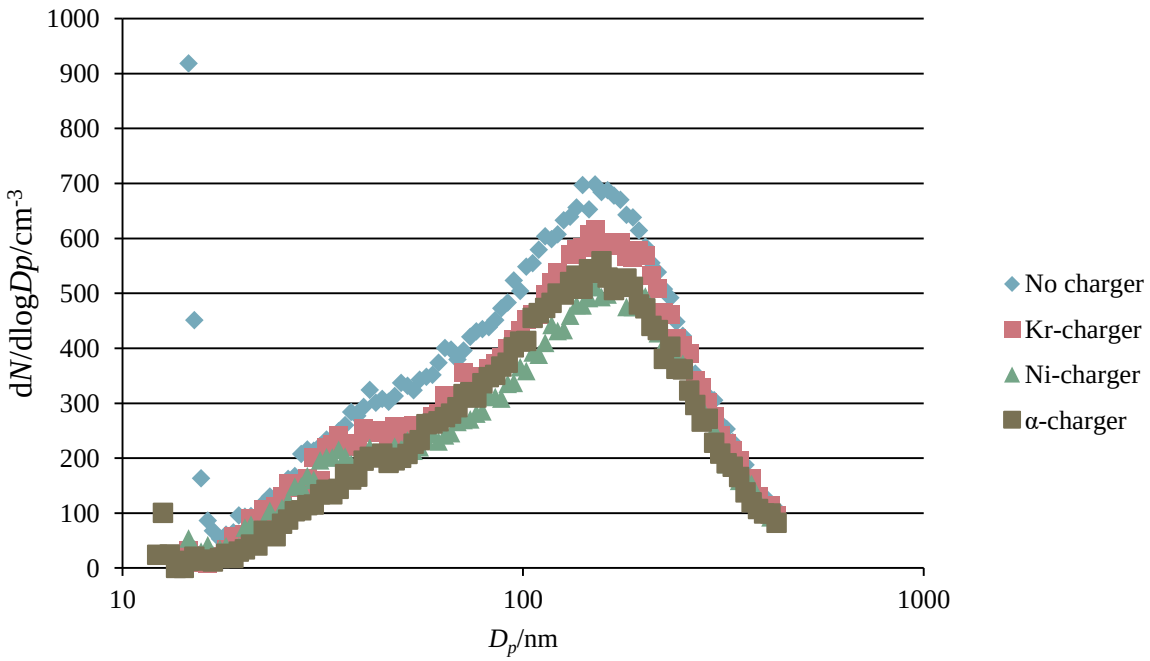

Figure 21. The average particle number size distribution where the α-charger contain 9 Am-sources. There are 10 measurements performed for each measurement sequence, and the average is calculated for these 10 measurements.

Figure 22 presents the results from the measurements with 15 Am-sources. Since the results with conventional Kr- and Ni-chargers shows similar results to the no charger experiment, we can conclude that, either the room air aerosol is already charged close to a bipolar charge distribution similar to after conventional chargers, or the Kr-charger and Ni-charger are not effective. The last hypothesis does not agree fully with our previous observations for 3 sources, since one of the hypothesis there was that the Kr-chargers and Ni-chargers are not effective, and that the Ni-charger is in addition leading to a loss of particles. We do not observe a loss of particles after the Ni-charger in the experiment with 15 Am-sources, why we find the explanation of losses in the Ni-charger as less likely. However, the explanation that the α-charger gives a too high charging state compared to conventional chargers explained in relation to 3 Am-sources can still hold. Again, it is plausible that the Am-sources give too intense charging of the particles, which leads to a too high particle number concentration as in Figure 17, at least if it is true that the charging state of the room air aerosol without chargers is similar to a bipolar distribution with conventional chargers.

Again, not knowing the charging state of the room air aerosol is severely affecting our ability to interpret the results. All in all, we cannot rule out also other plausible explanations of the behaviour during the different experiments.

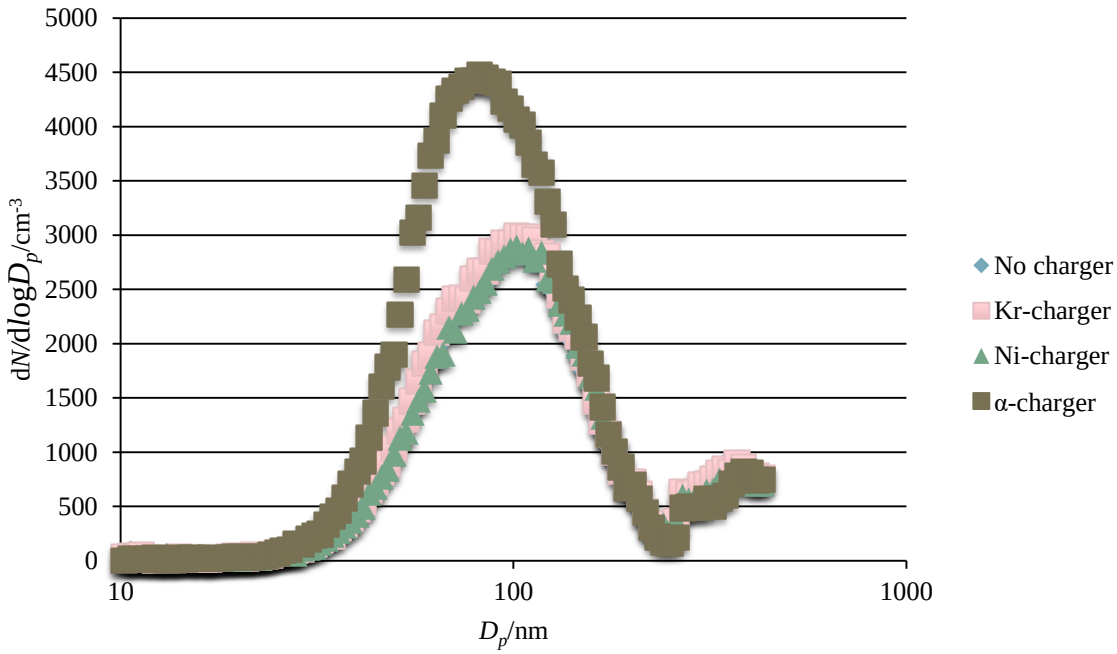

Figure 22. The average particle number size distribution where the α-charger contain 15 Am-sources. There are 10 measurements performed for each measurement sequence, and the average is calculated for these 10 measurements.

Discussion

Since the results of the measurements did not make it possible to answer the scientific questions presented in this thesis, the following discussion will concentrate on what the reason for this might be, but also what kind of methods that can be used to study this issue further.

The first problem that was recognized during the measurements was the difference between the conventional chargers. The Kr-charger and Ni-charger consist of two different radioactive substances; ^{85}Kr and ^{63}Ni. Since there is no documentation of when the radioactive substances are purchased, there is no way to estimate their half-life-time. This is not a worry for the Ni-charger, since it has a half-life of 100 years. The Kr-charger on the other hand has a lifetime of 10.8 years, which means that the radioactive substance is likely not effective anymore. Hence, this is likely the reason why the difference between measurements with no charger and the Kr-charger are not too far apart. We also speculated that the Ni-charger is very dirty and can have less charging and higher loss of particles, although we found this explanation less likely. To be on the safe side, we recommend a cleaning of the Ni-charger and measurements before and after cleaning to see if this affects the performance of the Ni-charger.

We could not conclude with certainty how the α-charger worked. One reason beside the possibility that we overcharge the particles as explained in the results section, is that we have an unsatisfactory geometrical construction of the α-charger holder. Further, the position of the Am-sources can also

affect whether α-charger is overcharging the particles or not. Figure 13 presents the interior of the α-charger, which is very different from both the Ni-charger and Kr-charger (Figure 23). The α-charger has 3 Am-sources that are glued to the bottom of the construction whilst both conventional chargers have radioactive sources hanging in the radioactive volume. Further, the inlet-flow and out-let flow pass partly in the same tube in the α-charger, which can cause disruption in the aerosol flow. These are some of the reasons why the construction of the α-charger should be re-considered.

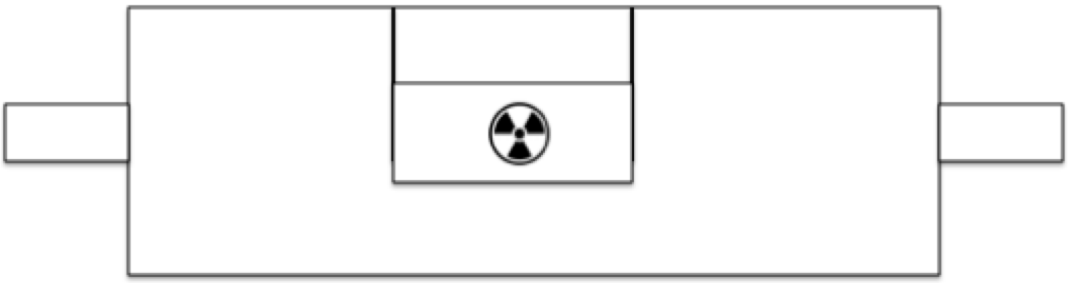

Figure 23. The interior of Ni-charger and Kr-charger. The figure was made by the author of this thesis (2018).

Further, the results did not show how many radioactive alpha sources are needed for a stable charge distribution, which is why there is a need of further studies. The measurements in this thesis were performed in a non-controlled laboratory environment, which contributed to high variation in the room air, both during one day and between the different measurement days. Different aerosol particles in the environment, for example new particle formation, or very aged particles in the accumulation mode might also give different charging state of the aerosol particles. Artificially produced particles in the lab would yield much more stable particle concentrations and particle types as suggested in the coming sub-sections.

Alternative 1 with nebulizer and electrospray

Figure 24 presents a schematic idea of the first alternative way to study the function of the α-charger. Polystyrene latex (PSL) particles are produced with a simple nebulizer and milliQ-water for particles above 200 nm diameters, or with an electro-spray generator for particles below 200 nm diameters. After production, the aerosol is dried with an aerosol diffusion drier. To be able to select particles of desired sizes (there will always be some particles present from the generator solution blow the desire sizes), they need to be charged with a charger of any kind. Further, the aerosols will pass through a DMA with a certain set voltage. Only single charged particles of the desired size are not selected by the DMA, since larger and smaller doubly charged particles are now produced in the generator. Hence, we know that there will only be particles of a single size and one charge. In the next step, we let the particles be charged by either no charger, the charger we would like to test, and/or a trustable charger before the air passes through a second DMA and finally a CPC. We scan all sizes with the second DMA. In this way, we can test how many single, doubly, and triple charged particles we have after the second DMA. By comparing the relation between the concentrations of single, doubly, and triply charged particles, we can see the proportion of these particles in the bipolar size distribution as function of the desired generated particle size. When the particles are not connected to a charger, we will get the total number concentration. In this way, we get the fraction of singly, doubly and triply charged particles in comparison to the total number concentration of particles. By placing a trustable charger between the first and second DMA, we can check that the experiments are performing in the desired way, or if there are losses which we need to take

into account. Even if the α-charger is not performing according to a known bipolar size distribution, it might still have its own charge distribution, which can be characterized in a controllable way.

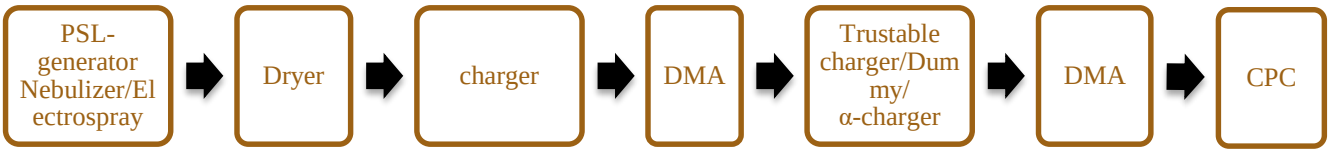

Figure 24. First suggestion of setup for future studies.

The difference between a nebulizer and electrospray is quite significant, depending on the desired generated particle size. The nebulizer will create a lot of particles of smaller sizes below the desired particle size in comparison to the electro spray generator. For this reason, a nebulizer can only be used for particles larger than 200 nm diameters. Figure 25 and 26 shows how a realistic and desired particle size distribution respectively will look like for particles generated with a nebulizer and milliQ-water. The electrospray produces relatively much smaller and fewer particles from the liquid solution, and hence can be used to study the charging distribution of particles down to about 20 nm diameters.

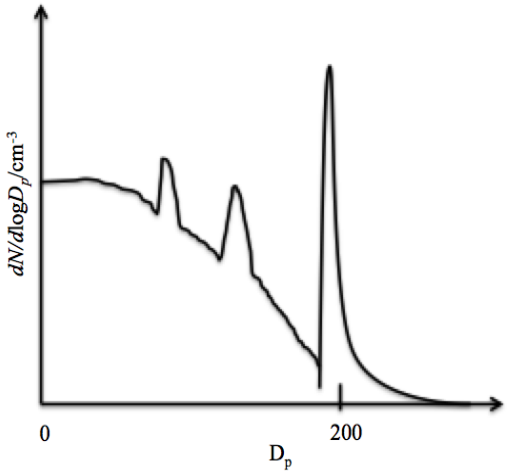

Figure 25. Realistic particle number size distribution for nebulizer generated particles with PSL spheres at 200 nm diameters. The figure was made by the author of this thesis (2018).

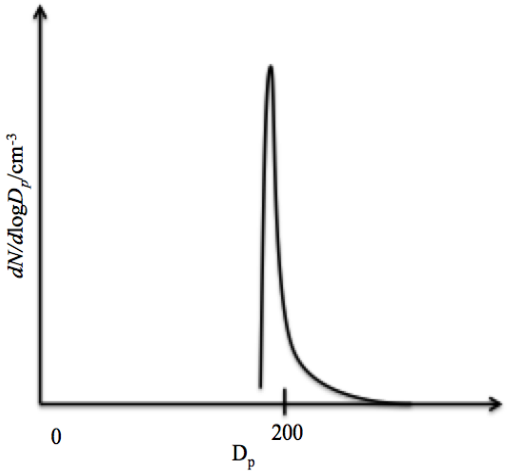

Figure 26. Hypothetical and desired particle number size distribution of nebulized particles, when there is no artefact of smaller sized milliQ-water particles. The figure was made by the author of this thesis (2018).

Alternative 2 with compressed air

There is another possibility for the set-up. It has a similar principle to the publication by Wiedensohler (1988), but with slight differences. It is presented in Figure 27. For this set-up, filtered compressed air is the starting point. After this step, the flow will pass through an oven, which contains a type of organic substance. When heated, the vapour will evaporate and later condense to form aerosol particles in the condenser, which are neutral due to the fact that the compressed air does not contain any ions.

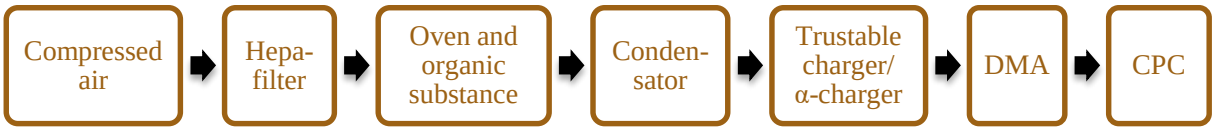

Figure 27. Second suggestion of setup for future studies.

Then, the particles are charged either to a known bipolar distribution with a trusted charger, or not charged (no charger), or charged by the Am-sources that we aim to test. After this, the size distribution is scanned by a DMA and particles counted by a CPC. By letting the air pass through the no-charger configuration, it is tested whether some particles pass through the DMA or not (the concentration in the CPC after passing through the DMA should be zero if no particles are charged). By letting the particles pass through the trusted charger, and comparing with the particles that pass through the α-

charger, it can be observed whether the Am-sources produce a different charging distribution in comparison with the trusted charger.

When doing measurements in lab or ambient air, there is a need of investigating the aerosol charge distribution. Buckley et al. (2008) presents an experimental set-up similar to the one used in this thesis, partly from the parallel DMA systems (Figure 28). Since it's a double set-up, one side runs the α-charger and measure aerosol particle size distribution. The other set-up will be without charger (neutrulizer) to measure aerosol mobility distribution. By combining the results from the two set-ups and recognized charge distribution equations, an estimation of the aerosol charge distribution can be performed.

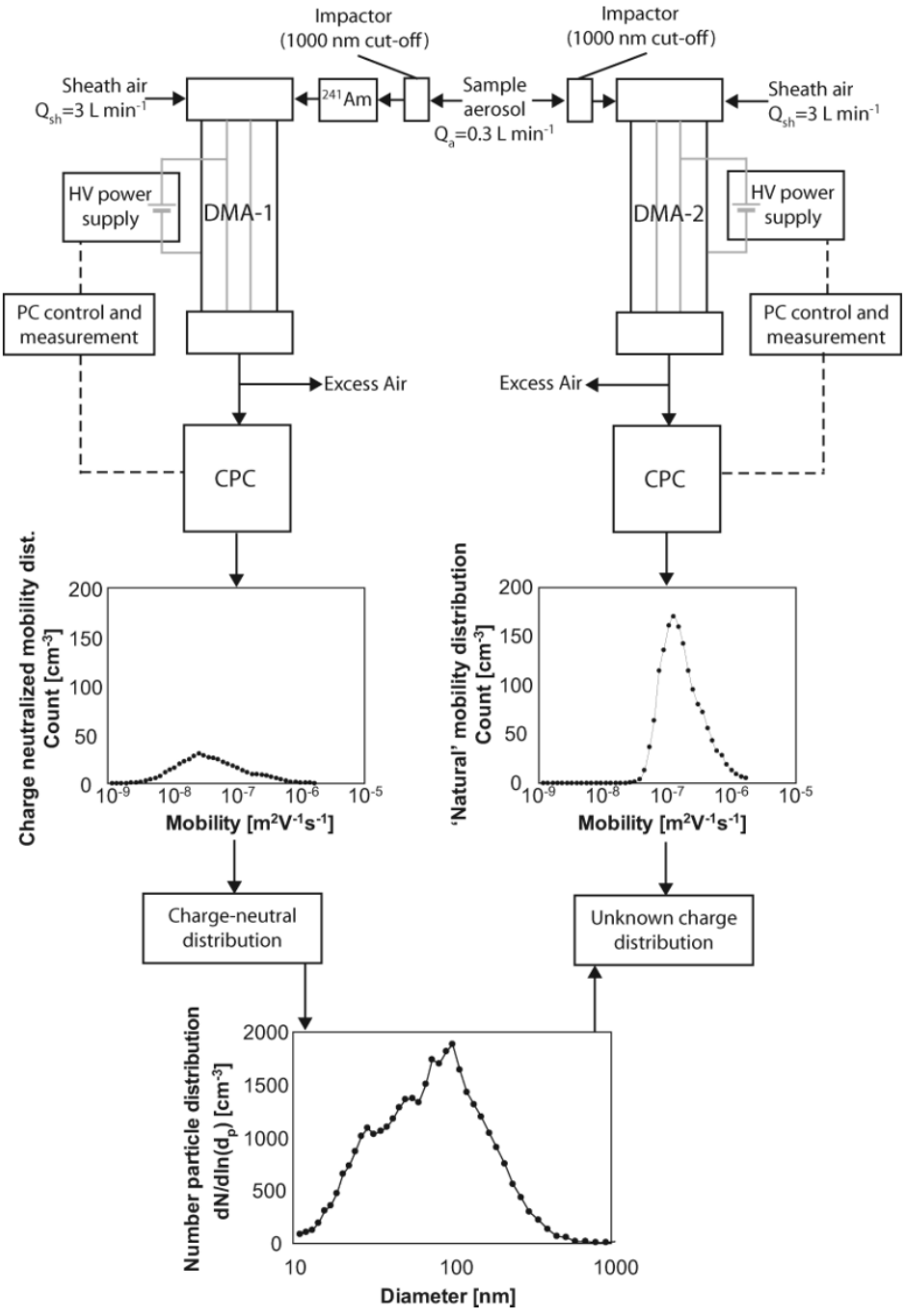

Figure 28. The double setup presented in Buckley et al. (2008). Permission to use by email.

Conclusions

The main conclusion from this thesis is that Am-sources could not be properly characterized. There is a likelihood that Am-sources give rise to a relatively higher charging than conventional chargers, but a definite answer to this question could not be achieved. After the experience gained by the current measurements, we suggest two alternative and rigorous methods, where aerosol production and charging state can be controlled when testing Am-sources. In other words, we cannot conclude if α-particles, such as in the α-charger system can be used as cost-effective alternative to perform SMPS measurements in nations with difficulties to attain radioactive chargers, and to characterize particles as function of size to investigate their climate and health effects.

References

Ahn, K-H., Kim, S-S. & Jeong, H-Y. 2005. *Condensation particle counter*. United States Patent.: US 6,980,284 B2.

Beckley, T.M., Martz, D., Nadeau, S., Wall, E. & Reimer, B. 2008. *Journal of Rural and Community Development.* 3 (3): 56-75. ISSN: 17128277.

Bhardawaj, A., Habib, G., Kumar, A., Singh, S & Kumar Nema, A. 2017. A review of ultrafine particle related pollution during vehicular motion, health effects, and control. *Journal of Environmental Science and Public Health.* 1(4): 268-288. DOI: 10.26502/jesph.96120024.

Boucher, O. 2015. Aerosol Modelling. *Atmospheric Aerosols: Properties and Climate Impacts.* Boucher, O. (.edt). Berlin, Germany: Springer. 51-81. ISBN: 9789401796484.

Bradshaw, B.C. 1951. The effect of grinding of particles. The Journal of Chemical Physics. 19 (8): 1057-1059. DOI: 10.1063/1.1748452.

Brown, R.C. 1997. Simultaneous measurement of particle size and particle charge. *Journal of Aerosol Science.* 28 (8): 1373-1391. DOI: 10.1016/S0021-8502(97)000347.

Buckley, A.J., Wright, M.D. & Henshaw, D.L. 2008. A Technique for Rapid Estimation of the Charge Distribution of Submicron Aerosols under Atmospheric Conditions. *Aerosol Science and Technology.* 42: 1042-1051. DOI: 10.1080/02786820802400645.

Colbeck, I. & Lazaridis, M. 2014. Introduction. *Aerosol Science: Technology and Applications*. Colbeck, I & Lazaridis, M (.edt) New Jersey: Wiley-Blackwell, 1-14. ISBN: 9781119977926.

Connan, O., Maro, D., Hérbert, D., Roupsard, P., Goujon, R., Letellier, B. & Cavelier, S. 2012. Wet and dry deposition pf particles associated metals (Cd, Pb, Zn, Ni, Hg) in a rural wetland site, Marais Vernier, France. *Atmospheric Environment.* 67: 394-403. DOI: 10.1016/j.atmosen.2012.11.029.

Dalirian, M. 2018. Investigating parameters governing liquid-phase cloud activation of atmospheric particles. Stockholms university. ISBN: 9789177971054.

DeMott, P., Sassen, K., Poellot, M.R., Baumgardner, D., Rogers, D.C., Brooks, S., Prenni, A.J. & Kreidenweis, S.M. 2003. African dust aerosols as atmospheric ice nuclei. *Geophysical Research Letters.* 30 (14): 424-442. DOI: 10.1029/2003GL017310.

Eisele, F.L. 1989. Natural and anthropogenic negative ions in the troposphere. *Journal of Geophysical Research.* 94 (D2): 2183-2196. DOI: 10.1029/JD094iD02p02183.

Flagan, R.C. & Seinfeld, J.H. 1988. Aerosols. *Fundamentals of air pollution engineering.* New Jersey, USA: Prentice-Hall Inc. 290-356. ISBN: 0133325377.

Friedlander, S.K. 1977. Smoke, dust and haze: Fundamentals of aerosol behaviour. *Physics today.* 30 (9): 58-59. DOI: 10.1063/1.3037714.

Fröhlich-Nowoisky, J., Kampf, C.J., Weber, B., Huffman, J.A., Pöhlker, C., Andreae, M.O., Lang-Yona, N., Burrows, S.M., Gunthe, S.S., Elbert, W., Su, H., Hoor, P., Thines, E., Hoffmann, T., Després, V.R. & Pöschl, U. 2016. Bioaerosols in the Earth system: Climate, health, and ecpsystem indicators. *Atmospheric Research.* 182: 346-376. DOI: 10.1016/j.atmosres.2016.07.018.

Fuchs, N.A. 1963. On the stationary charge distribution on aerosol particles in a bipolar ionic atmosphere. *Geofisica pura e applicata.* 56 (1): 185-193. DOI:10.1007/BF01993343.

Fullova, D & Durcanska, D. 2016. Laboratory measurements of particulate matter concentrations from asphalt pavement abrasion. *De Gruyter*. 12 (2/2016): 94-102. DOI: 10.1515/cee-2016-0013.

Gunn, R. 1955. The Statistical Electrification of Aerosols by Ionic Diffusion. *Journal of Colloid Science.* 10 (1): 107-119. DOI: 10.1016/0095-8522(55)90081-7.

Gustafsson, M., Blomqvist, G., Gudmundsson, A., Dahl, A., Jonsson, P. & Swietlicki, E. 2009. Factors influencing PM10 emissions from road pavement wear. *Atmospheric Environment.* 43 (31): 4699-4702. DOI: 10.1016/j.atmosenv.2008.04.028.

Hill, T.C.J., Moffett, B.F., DeMott, P.J., Georgakopoulos, D.G., Stump, W.L. & Franc, G.D. 2014. The measurements of Ice Nucleation-Active Bacteria on plants and in precipitation by Quantitative PCR. *Applied and Environmental Microbiology.* 80 (4): 1256-1267. DOI: 10.1128/AEM.02967-13.

Hemond, H. F. & Fechner, E. J. 2015. The Atmosphere. *Chemical fate and transport in the environment.* Hemond, H.F. & Fechner, E. J (.edt). San Diego: Academic Press Inc, 311-454. DOI: 10.1016/B978-0-12-398256-8,00004-9.

Hochrainer, D. 1985. Measurement methods for electic charges on aerosols. *The Annals of Occupational Hygiene.* 29 (2): 241-249. DOI: 10.1093/annhygg/29.2.241.

Hoppel, W.A & Frick, G.M. 1986. Ion-Aerosol attachment coefficients and the steady-state charge distribution on Aerosols in a Bipolar ion environment. *Aerosol Science and Technology.* 5 (1): 1-21. DOI: 10.1080/02786828608959073.

Hussein, A., Scheibel, H.G., Becker, K.H. & Porstendörfer, J. 1983. *Journal of Aerosol Science.* 14: 671-678. DOI: 10.1016/0021-8503(83)90071-X.

Institute of Atmospheric and Climate science. W.Y. *Differential Mobility Particle Sizer (Aerosol measurements).* Zurich. URL: https://www.ethz.ch/content/dam/ethz/special-interest/usys/iac/iac-dam/documents/edu/courses/atmospheric_physics_lab_work/DMPS_en_2014.pdf [2018-05-13].

Jacobson, M.Z. & Turco, R.P. 1995. Simulating Condensational growth, evaporation, and coagulation of aerosols using a combined moving and stationary size grid. *Aerosol Science and Technology.* 22 (1): 73-92. DOI: 10.1080/02786829408959729.

Jin Ma, C. & Yamamoto, M. 2015. Artificial and Bilogical Particles in Urban Atmosphere. *Current Air Quality Issues*. Nejadkoorki, F (.edt). New York, USA:

Springer Open Book: 203-217. ISBN: 9789535121800.

Johansson, L.S., Tullin, C., Leckner, B. & Sjövall, P. 2003. Particle emissions from biomass combustion in small combustors. *Biomass and Bioenergy.* 25 (4): 435-446. DOI: 10.1016/S0961-9534(03)00036-9.

Jones, A.M. & Harrison, R.M. 2014. The effects of meteorological factors on atmospheric bioaerosols concentration – a rewiew. *Science of the total environment.* 326 (1-3): 151-180. DOI: 10.1016/j.scitotenv.2003.11.021.

Karydis, V.A., Tsimpidi, A.P., Bacer, S., Pozzer, A., Nenes, A. & Lelieveld, J. 2017. Global impact of mineral dust on cloud droplet number concentration. *Atmospheric, Chemistry and Physics.* 17: 5601-5621. DOI: 10.5194/acp-17-5601-2017.

Knutson, E.O. 1976. Extended elecric mobility for measuring aerosol particle size and concentration. *Fine Particles: Aerosol Generation, Measurement, Sampling and Analysis.* Liu, B.Y.H (.edt) New York, USA: Elservier Inc. ISBN: 9780124529502.

Kok, J.F., Parteli, E.J.R., Michaels, T. & Bou Karam, D. 2012. The physics of wind-blown sand and dust. *Earth and Planetary Astrophysics.* 75 (10): 106901. DOI: 10,1088/0034-4885/75/10/106901.

Kristensson, A. 2018. Brownian diffusion. [Private communication].

Kulkarni, P., Baron, P. & Willeke, K. 2011. Fundamentals of Single Particle Transportation. *Aerosol Measurements: Principles, Techniques and Applications.* Kulkarni, P., Baron, P. & Willeke, K. (.edt) New Jersey, USA: Wiley-Blackwell,15-30. ISBN: 9780470387412.

Kulmala, M., Kontkanen, J., Junninen, H., Lehtipalo, K., Manninen, H., Nieminen, T.,Petäjä, T., Sipilä, M., Schobesberger, S., Rantala, P., Franclin, A., Jokinen, T., Järvinen, E., Äijälä, M., Kangasluoma, J., Hakala, ., Aalto, P., Paasonen, P., Mikkilä, J., Vanhanen, J., Aalto, Hakola, H., Makkonen, U., Ruuskanen, T., Mauldin III, R., Duplissy, J., Vehkamäki, H., Bäck, J., Kortelainen, A., Riipinen, I., Kurtén, T., Johnston, M., Smith, J., Ehn, M., Mentel, T., Lehtinen, K., Laaksonen, A., Kerminen, V-M. & Worsnop, D. 2013. Direct observations of atmospheric aerosol nucleation. *Science.* 339 (6122): 943-946. DOI: 10.1126/science.1227385.

Lagzi, I., Mészáros, R., Gelybó, G., Leelössy, Á., 2013. Atmospheric Chemistry. A book, being part of the project entitled "E-learning scientific content development in ELTE TTK" with number TÁMOP-4.1.2.A/1-11/1-2011-0073, Eötvös Loránd University. URL://elte.prompt.hu/sites/default/files/tananyagok/AtmosphericChemistry/ [2018-03-16].

Leppä, J. 2012. Dynamics of neutral and charged aerosol particles. *Journal of Aerosol Science*. 137. ISBN: 978952-5822-66-3.

Lohmann, U., Luönd, F. & Mahrt, F. 2016. Thermodynamics. Lohmann, U., Luönd, F. & Mahrt, F (.edt). Cambridge, United Kingdom: Cambridge University Press. 26-67. ISBN: 9781107018228.

Mahowald, N., Albani, S., Kok, J.F., Engelstaeder, S., Scanza, R., Ward, D.S. & Flanner, M.G. 2014.The size distribution of desert dust aerosols and its impact on Earth system. *Aeolian Research*. 15: 53-71. DOI: 10.1016/j.aeolia.2013.09.002.

McFiggans, G., Artaxo, P., Baltensperger, U., Coe, H., Facchini, M.C., Feingold, G., Fuzzi, S., Gysel, M., Laaksonen, A., Lohmann, U., Mentel, T.F., Murphy, D.M., O'Dowd, C.D., Snider, J.R. & Weingartner, E. 2006. The effect of physical and chemical aerosol properties on warm cloud droplet activation. *Atmospheric, Chemistry and Physics.* 6: 2593-2649. DOI: 10.5194/acp-6-2593-2006.

Millikan, R.A., Gottschalk, V.H. & Kelly, M.J. 1920. The nature of the process of ionization of gases by alpha rays. *The physical review.* 15 (3): 157-177. DOI: 10.1103/PhysRev.15.157.

Mohan, S. 2015. An overview of particulate dry deposition: measuring methods, deposition velocity and controlling factors. *Environment, Science and Technology.* 13: 387-402. DOI: 10,1007/s13762-015-0898-7.

Ounis, H., Ahmadi, G. & McLaughlin, J.B. 1991. Dispersion and Deposition of Brownian Particles from Point Sources in a Simulated Turbulent Channel Flow. *Journal of Colloid and Interface Science.* 147 (1): 233-250. DOI: 10.1016/0021979790151-W.

Pettibone, A.J. 2009. Toward a better understanding of new particle formation. Thesis, University of Iowa. URL:https://ir.uiowa.edu/cgi/viewcontent.cgi?article=1605 &context=etd [2018-03-16].

Querol, X., Alastuey, A., Viana, M.M., Rodrigues, S., Artinano, B., Salvador, P., Garcia do santos, S., Fernandez Patier, R., Ruiz, C.R., de la Rosa, J., Sanchez de la Campa, A., Menendez, M. & Gil, J.I. 2004. Speciation and origin of PM10 and PM2.5 in Spain. *Journal of Aerosol Science.* 35 (9): 1151-1172. DOI: 10.1016/j.jaerosci.2004.04.002.

Ruijgrok, W., Davidson, C. & Nicholson, K. 1995. Dry deposition of particles, Implications and recommendations for mapping of deposition over Europe. *Tellus.* 47B: 587-501. ISSN: 0280-6509.

Salou, M., Siffert, B. & Jada, A. 1998. Study of the stability of bitumen emulsions by application of DLVO theory. *Colloids and Surfaces A: Physicochemical and Engineering Aspects.* 142 (1): 9-16. DOI: 10.1016/S0927-7757(98)00406-3.

Seinfeld, J. & Spyros, P. 2006. Atmospheric Chemistry. *Atmospheric Chemistry and Physics: From air pollution to climate change.* New Jersey, USA: Wiley, 69-87. ISBN: 9781119221166.

Shimada, M., Matsuska, S. & Masuda, H. 2006. Fundamental properties of particles. Masuda, H., Highasitani, K. & Yoshida, H. (.edt). Florida, USA: CRC Press. 103-244. ISBN: 9781574447828.

Smirnov, B.M. 2017. Charged Particles in Atmosphere. *Microphysics of Atmospheric Phenomena.* New York, USA: Springer Publishing Company, 35-57. ISBN: 9783319308135.

Sorjamaa, R. & Laaksonen, A. 2007. The effect of H_2O adsorption on cloud drop activation of insoluble particles: a theoretical framework. *Atmospheric, Chemistry and Physics.* 7 (24): 6175-6180. DOI: 10.5194/acp-7-6175-2007.

The university of Manchester. 2017. Center for atmospheric science: Condensation particle counter (CPC). URL:http://www.cas.manchester.ac.uk/restools/instruments/aerosol/cpc/ [2018-04-26].

Tomasi, C., & Lupi, A. 2016. Primary and Secondary sources of Atmospheric Aerosol. *Atmospheric aerosols: Life cycles and effect on air quality and climate.* Tomasi, C., Fuzzi, S. & Kokhanovsky, A. (.edt) New Jersey, USA: Wiley, 1-86. ISBN: 9783527336456.

Verheggen, B. & Weijers, E.P. 2010. *Climate change and the impact of aerosol.* Energy research centre of the Netherlands. URL:https://www.ecn.nl/publications/PdfFetch.aspx?nr=ECN-E--09-095 [2018-05-13].

Wagner, P.E. 1982. Aerosol growth by condensation. *Aerosol Microphysics II. Topics in current physics.* Marlow, W.H (.edt) Berlin, Germany. ISBN: 9783642818073.

Wang, X., Deane, G.B., Moore, K.A., Ryder, O.S., Stokes, M.D., Beali, C.M., Collins, D.B., Santander, G.B., Burrows, S.M., Sultana, C.M. & Prather, K.A. 2017. The role of jet and film drops in controlling the mixing state of submicron sea spray aerosol particles. *Proceedings of the National Academy of Sciences of the United States of America.* 114 (27): 6978-6938. DOI: 10.1073/pnas.1702420114.

WHO, 2017. Air pollution. URL: http://www.who.int/airpollution/en/ [2018-04-12].

Wichmann, H-E. 2007. Diesel exhaust particles. *Inhalation Toxicology.* 19 (1): 241-244. DOI: 10.1080/08958370701498075.

Wiedensohler, A. 1988. An approximation of the bipolar charge distribution for particles in the submicron size range. *Journal Aerosol science.* 19 (3): 387-389. DOI: 0021-8502/88.

Wilson, T.W., Ladino, L.A. Alpert, P.A., Breckles, M.N., Brooks, I.M., Browse, J., Burrows, S.M., Carslaw, K.S., Huffman, A., Judd, C., Kilthau, W.P., Mason, R.H., McFiggans, G., Miller, L.A., Nájera, J.J., Polishchuk, E., Rae, S., Schiller, C.L., Si, M., Temprado, J.V., Whale, T.F., Wong, J.P.S., Wurl, O., Yakobi-Hancook, J.D., Abbatt, J.P.D., Aller, J.Y., Bertram, A.K., Knopf, D.A. & Murray, B.J. 2015. A marine biogenic source of atmospheric ice-nucleating particles. *Nature, international journal of Science.* 525: 234-238. DOI: 10.1038/nature14986.

Zhang, J & Shao, Y. 2014. A new parameterization of particle dry deposition over rough surfaces. *Atmospheric, Chemistry and Physics.* 14: 12429-12440. Doi: 10.5194/acp-14-12429-2014.

Zhang, R., Jing, J., Tao, J., Hsu, S.-C., Wang, G., Cao, J., Lee, C.S.L., Zhu, L., Chen, Z., Zhao, Y. and Shen, Z. 2013. Chemical characterization and source apportionment of $PM_{2.5}$ in Beijing: seasonal perspective. *Atmospheric, Chemical and Physics.* 13: 7053-7074. DOI: 10.5194/acp-13-7053-2013.

Zhou, J. 2001. Hygroscopic properties of atmospheric aerosol particles in various environments. Doctoral dissertation. ISBN: 9178741203. Lunds University, Lund, Sweden.

Attachment 1 – 3 Am-sources

Figure 3a-3j presents the results from the 10 particle number size distribution measurements in the 4-step measurement sequence belonging to Figure 19 with 3 Am-sources.

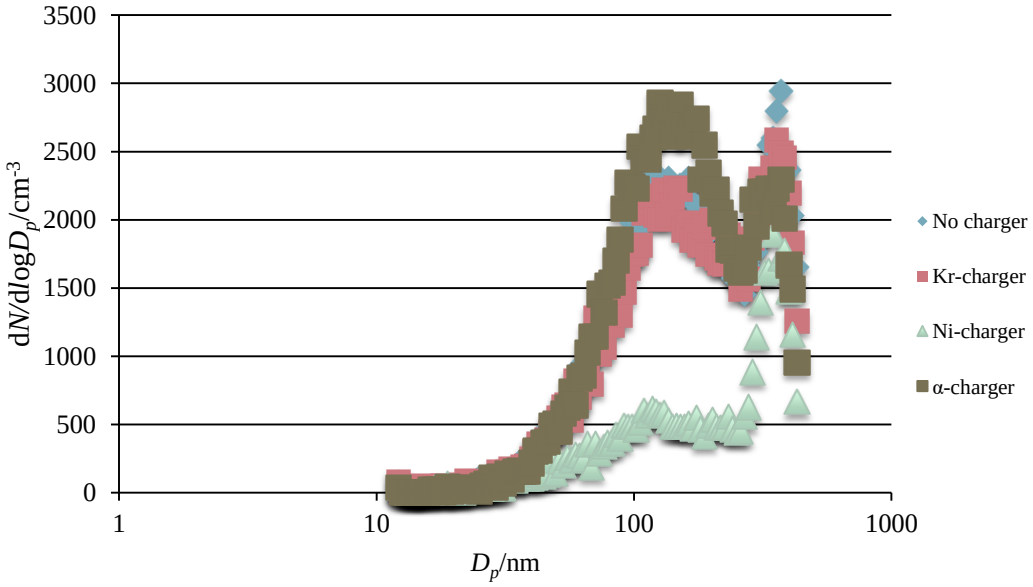

Figure 3a. The first measurement where the α-charger contains 3 Am-sources.

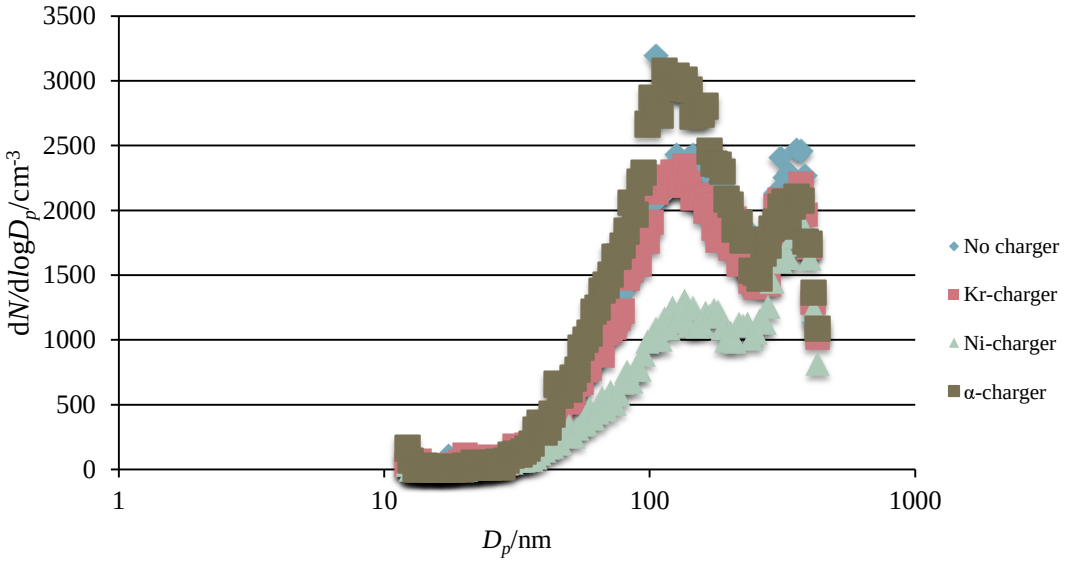

Figure 3b. The second measurement where the α-charger contains 3 Am-sources.

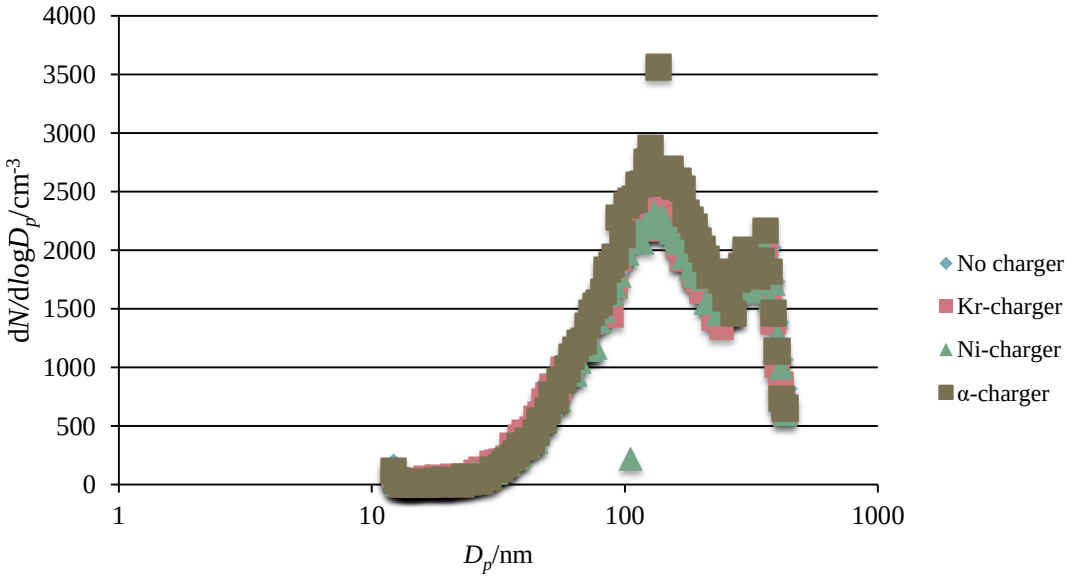

Figure 3c. The third measurement where the α-charger contains 3 Am-sources.

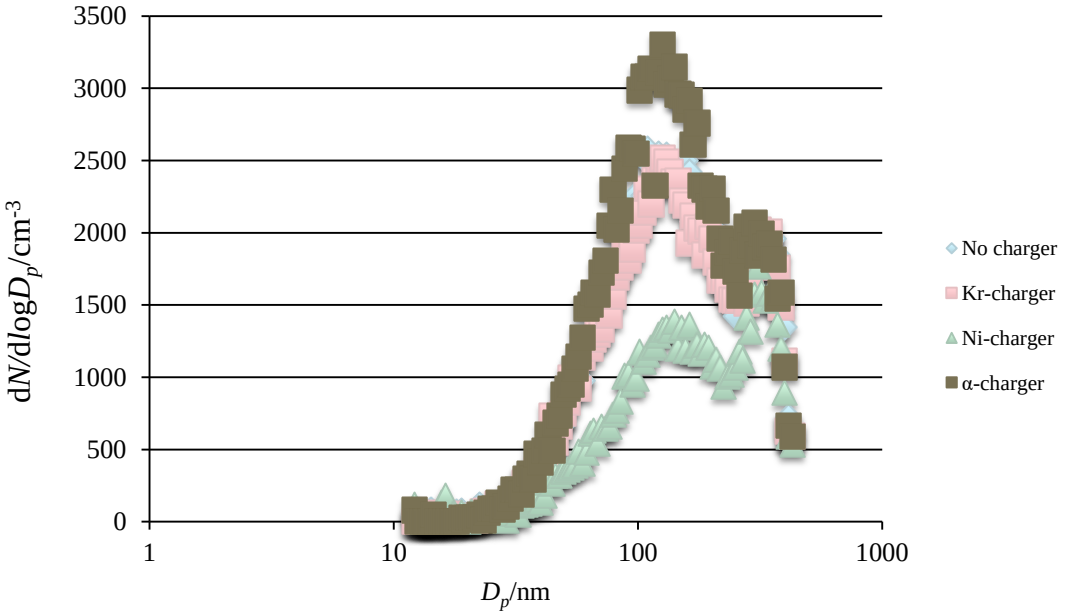

Figure 3d. The fourth measurement where the α-charger contains 3 Am-sources.

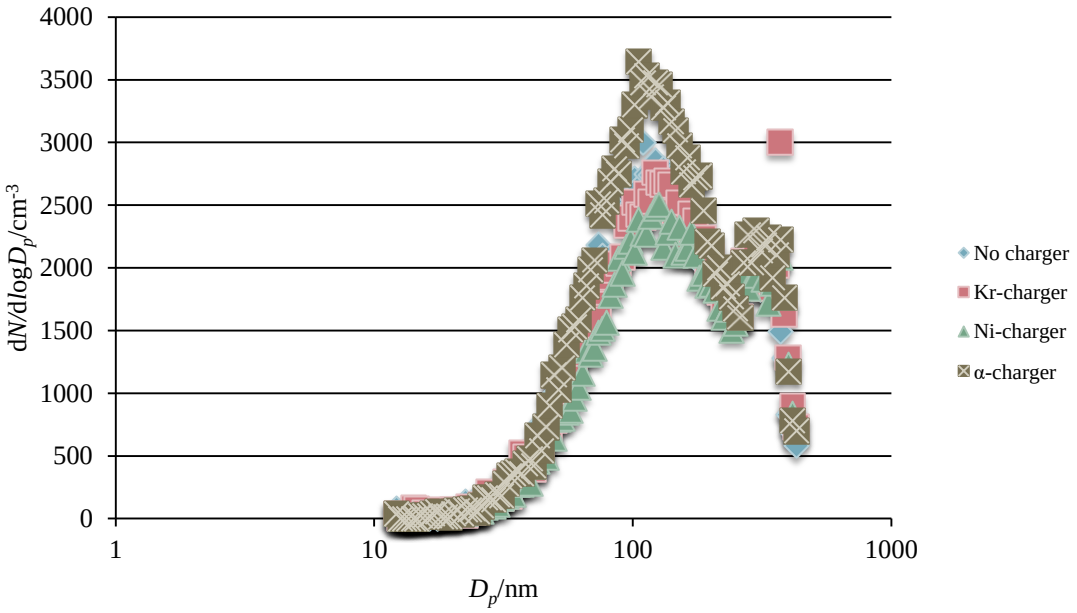

Figure 3e. The fifth measurement where the α-charger contains 3 Am-sources.

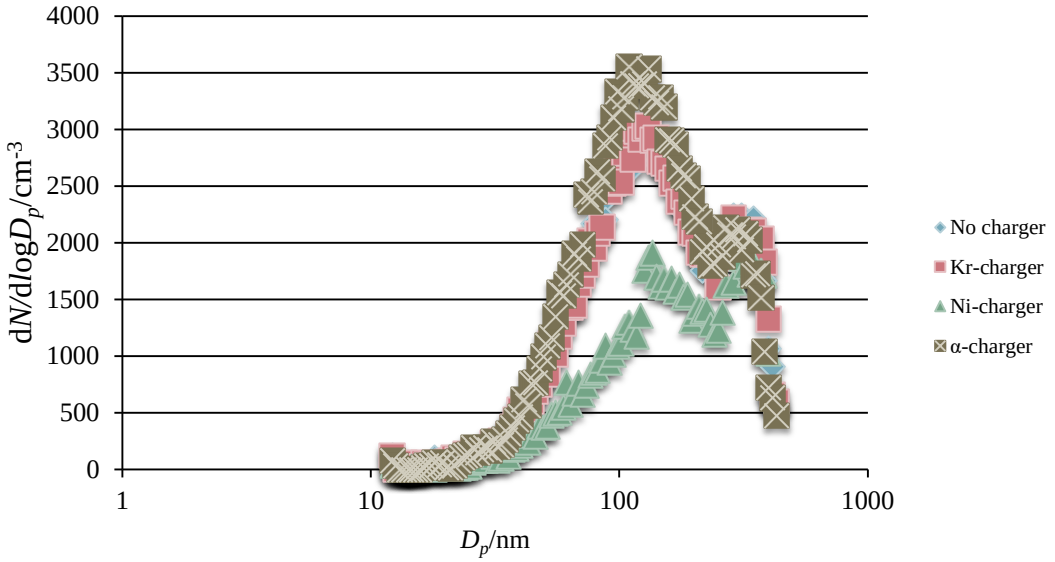

Figure 3f. The sixth measurement where the α-charger contains 3 Am-sources.

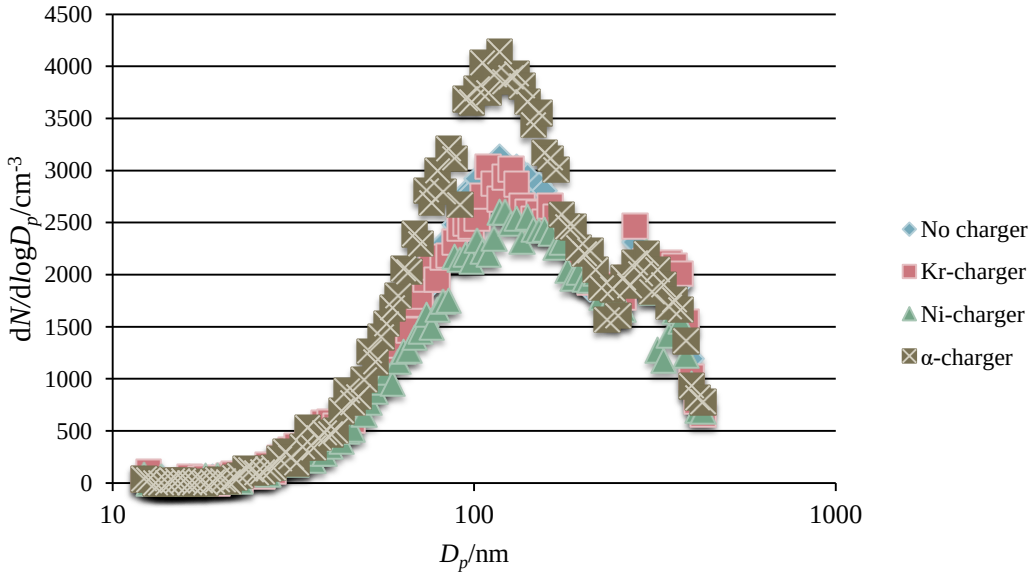

Figure 3g. The seventh measurement where the α-charger contains 3 Am-sources.

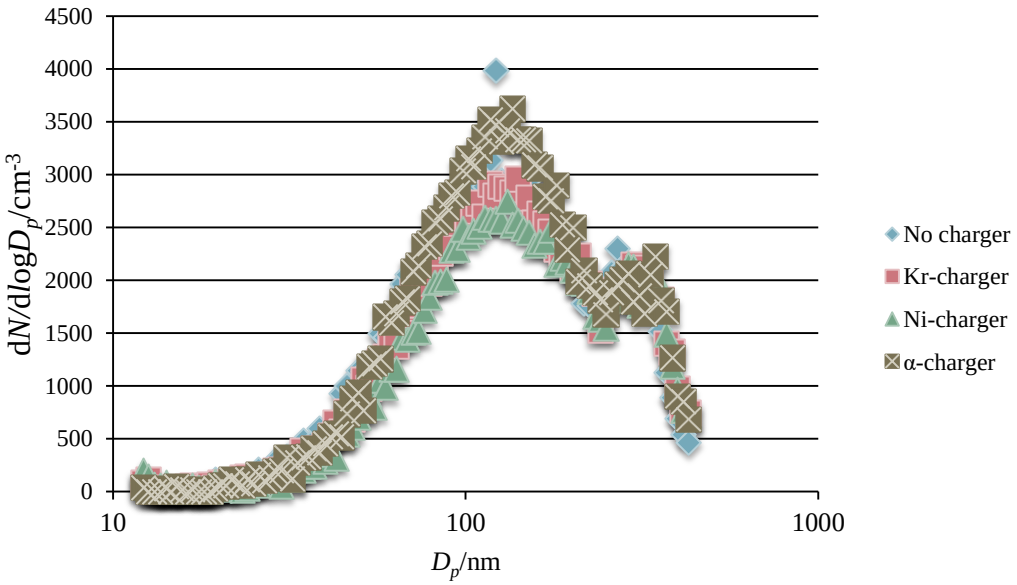

Figure 3h. The eight measurement where the α-charger contains 3 Am-sources.

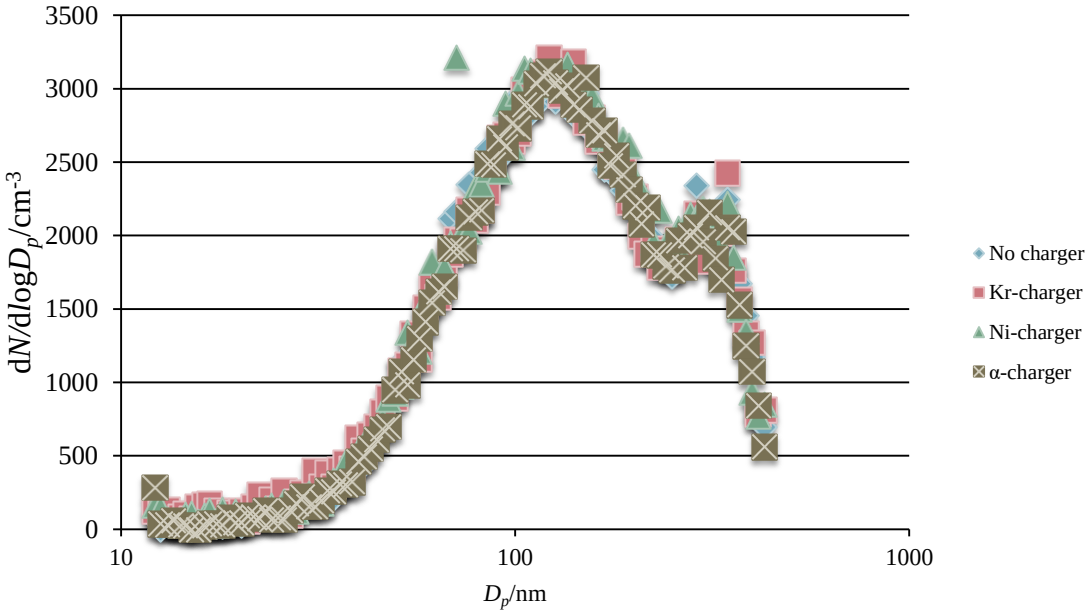

Figure 3i. The nine measurement where the α-charger contains 3 Am-sources.

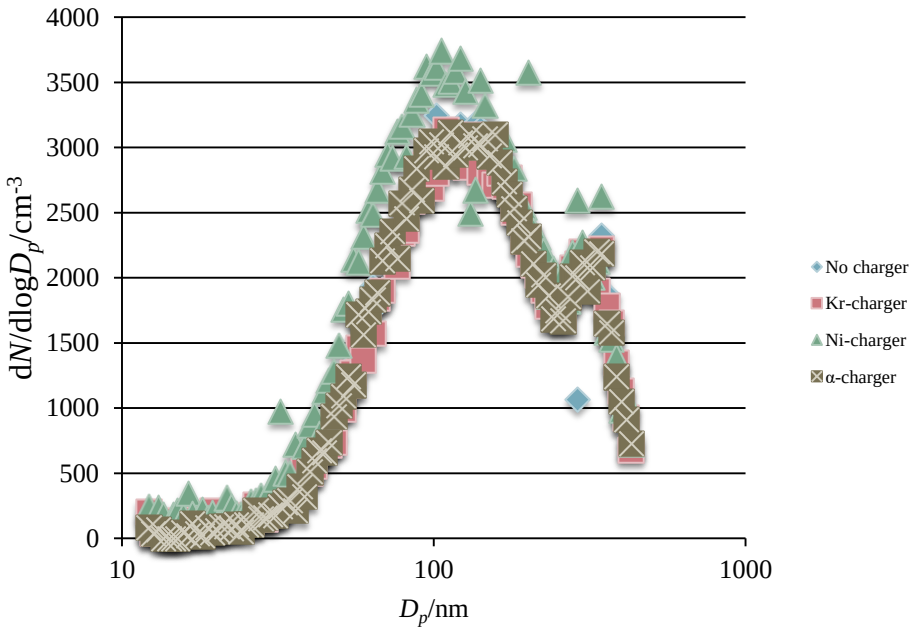

Figure 3j. The tenth measurement where the α-charger contains 3 Am-sources.

Attachment 2 – 7 Am-sources

Attachment 2 presents the measured particle number size distribution for the 10 measurements with 7 Am-sources in the 4 step measurement sequence.

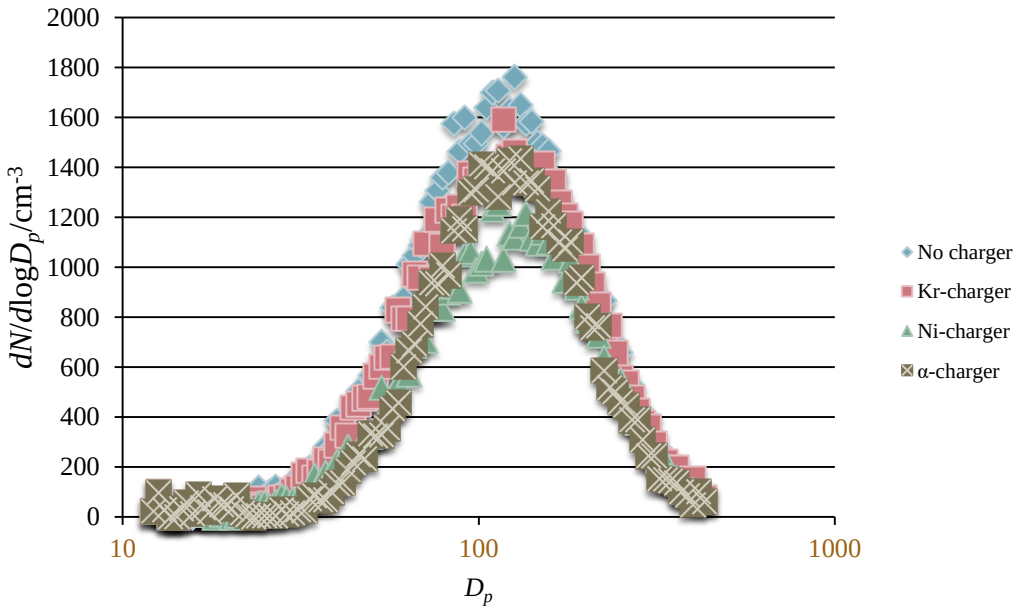

Figure 7a. The first measurement where the α-charger contains 7 Am-sources.

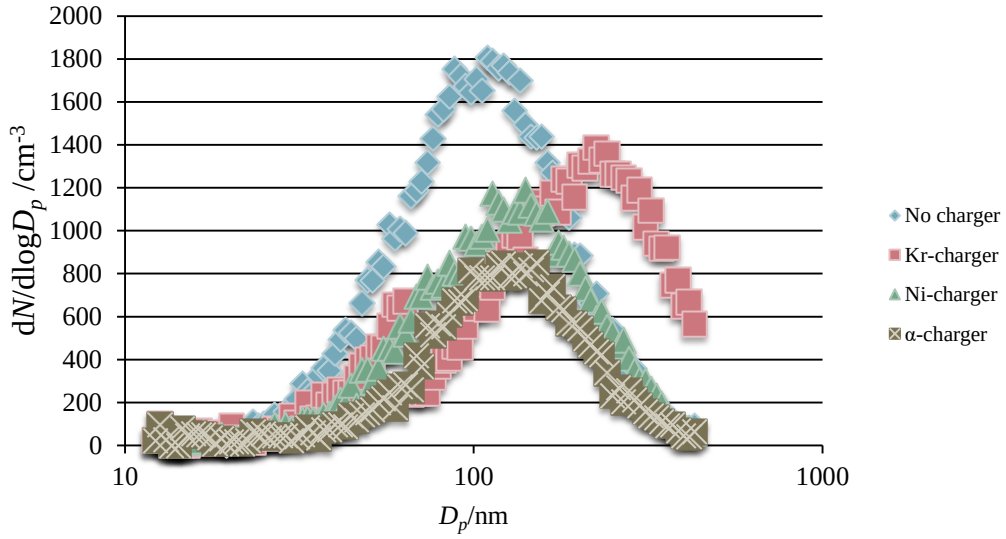

Figure 7b. The second measurement where the α-charger contains 7 Am-sources.

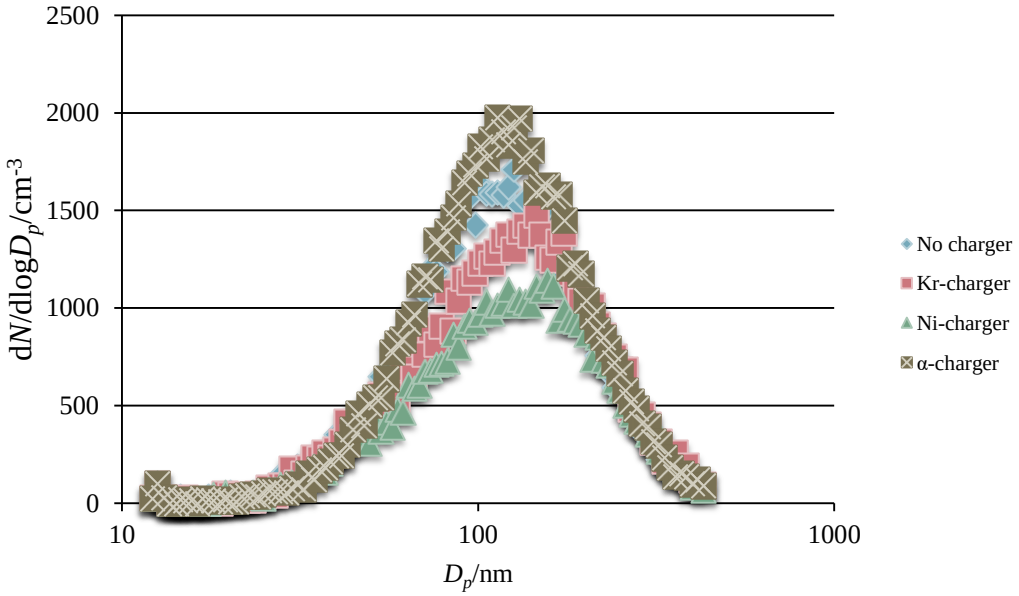

Figure 7c. The third measurement where the α-charger contains 7 Am-sources.

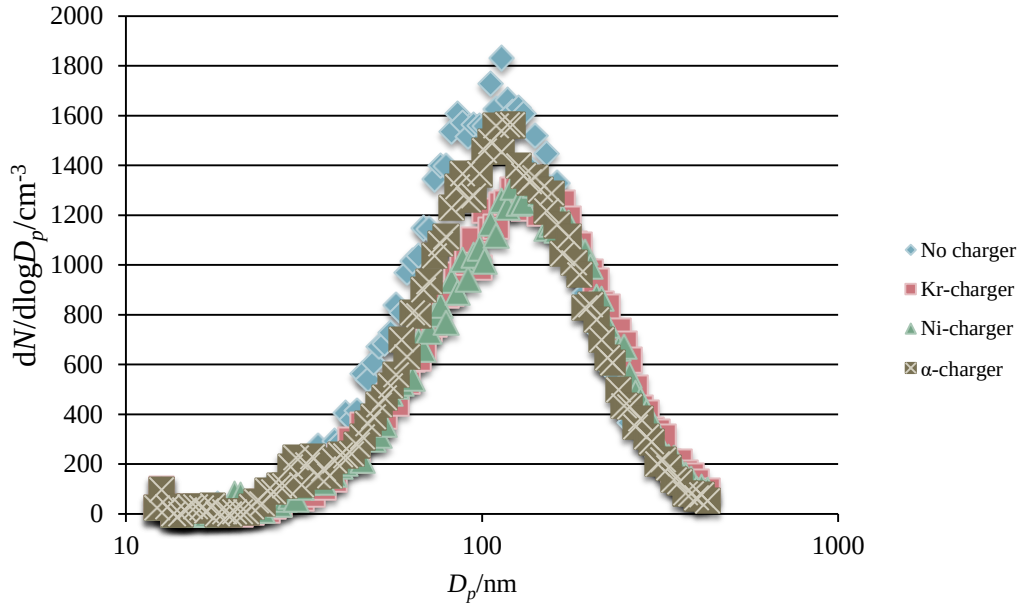

Figure 7d. The forth measurement where the α-charger contains 7 Am-sources.

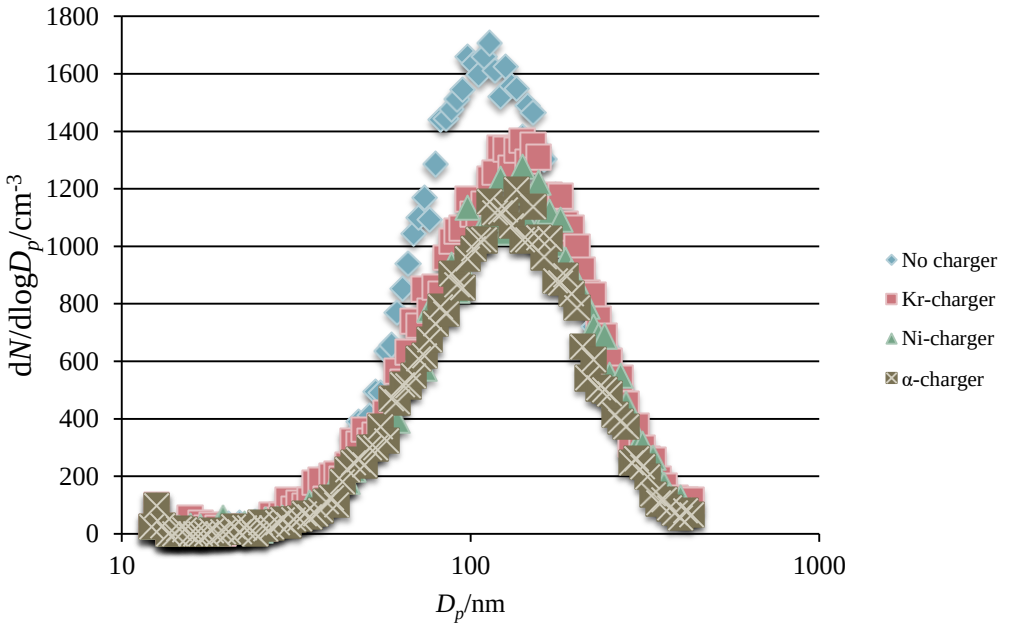

Figure 7e. The fifth measurement where the α-charger contains 7 Am-sources.

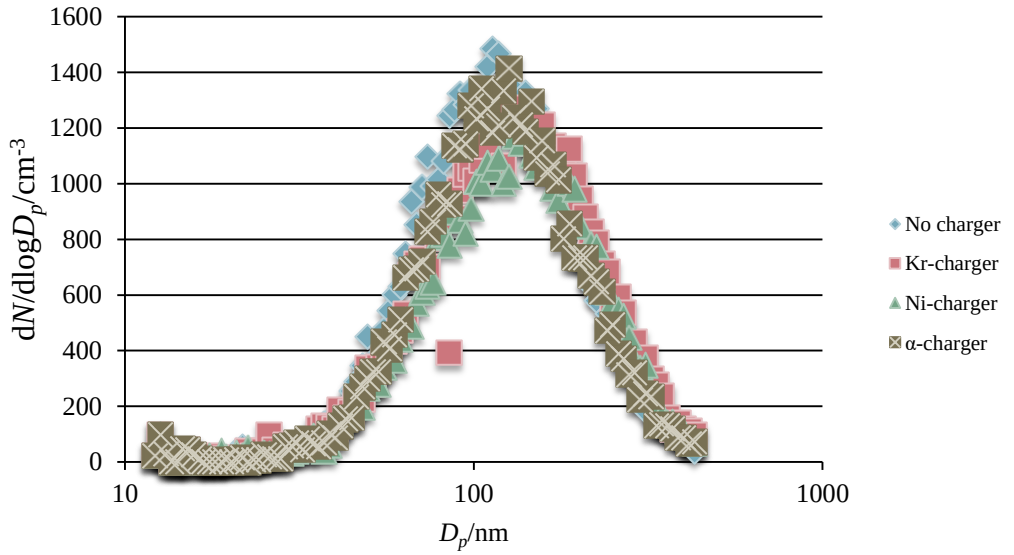

Figure 7f. The sixth measurement where the α-charger contains 7 Am-sources.

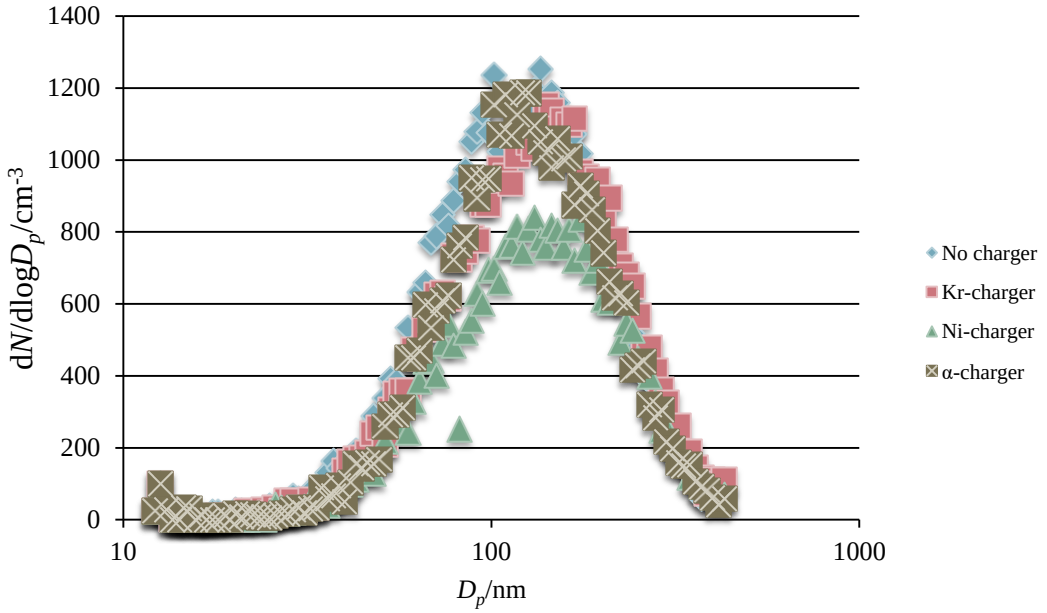

Figure 7g. The seventh measurement where the α-charger contains 7 Am-sources.

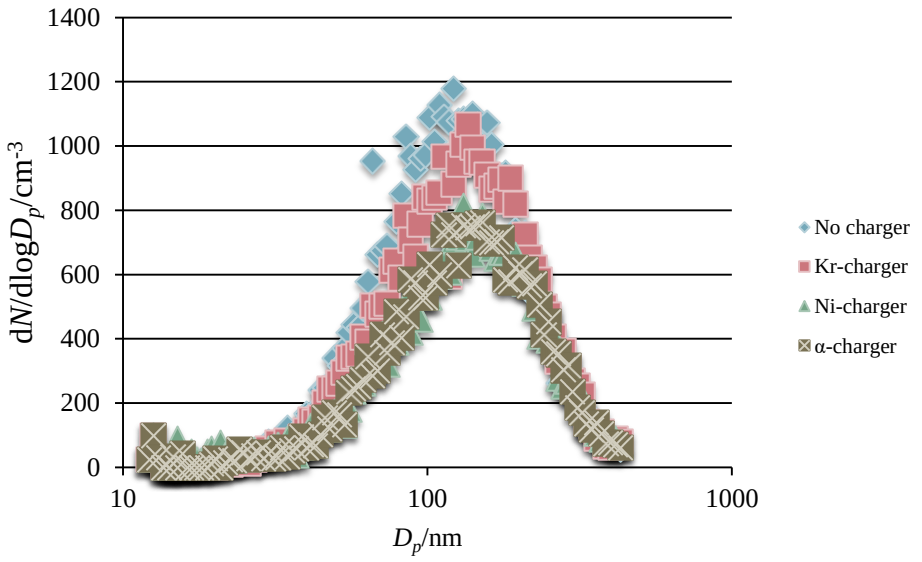

Figure 7h. The eight measurement where the α-charger contains 7 Am-sources.

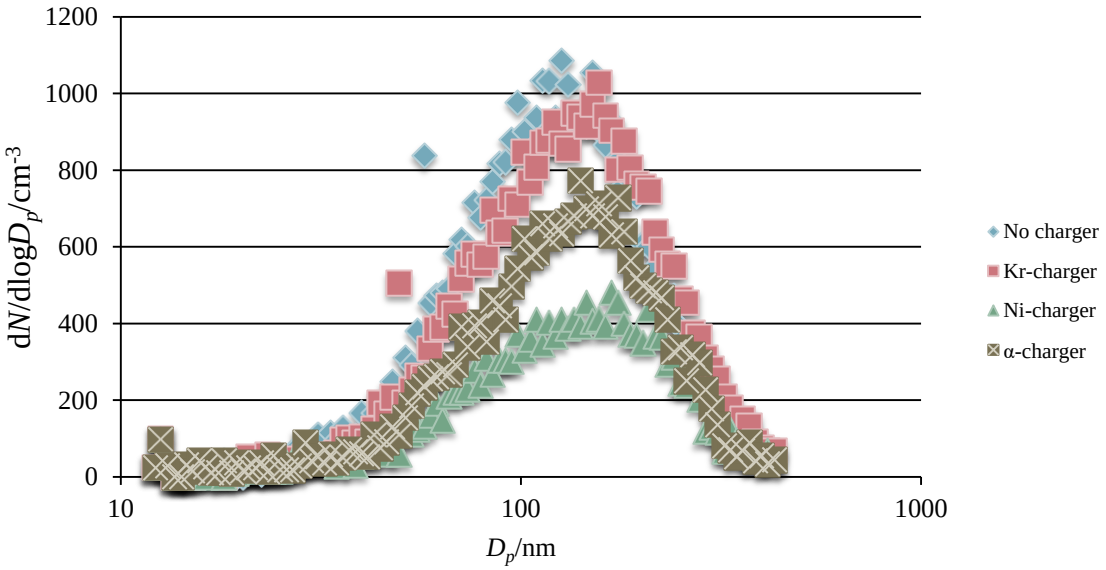

Figure 7i. The ninth measurement where the α-charger contains 7 Am-sources.

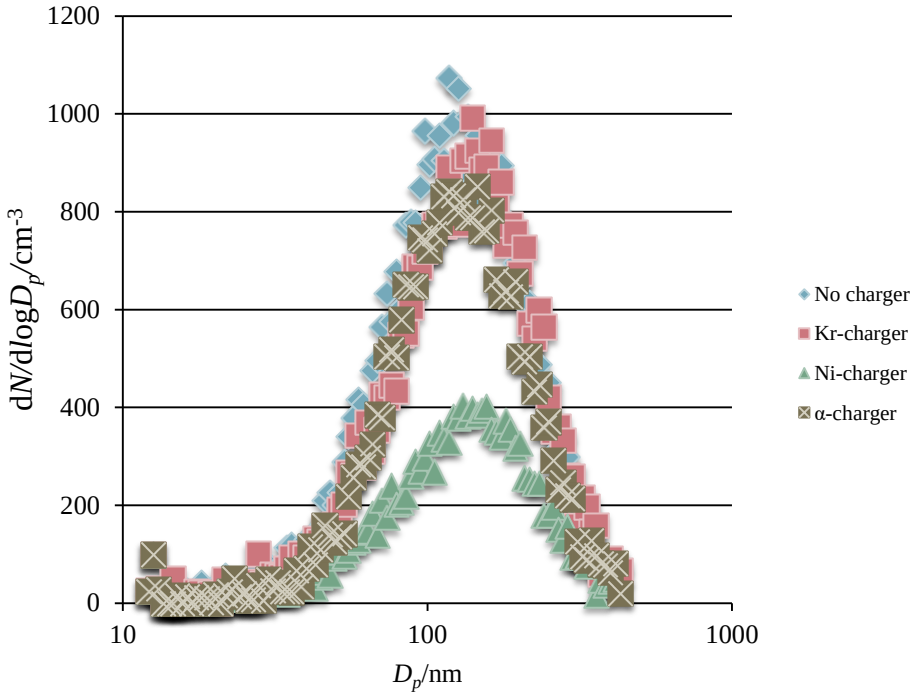

Figure 7j. The ninth measurement where the α-charger contains 7 Am-sources.

Attachment 3 – 9 Am-sources

Attachment 3 presents the measured particle number size distribution for the 10 individual measurements with 9 Am-sources in the 4 step measurement sequence.

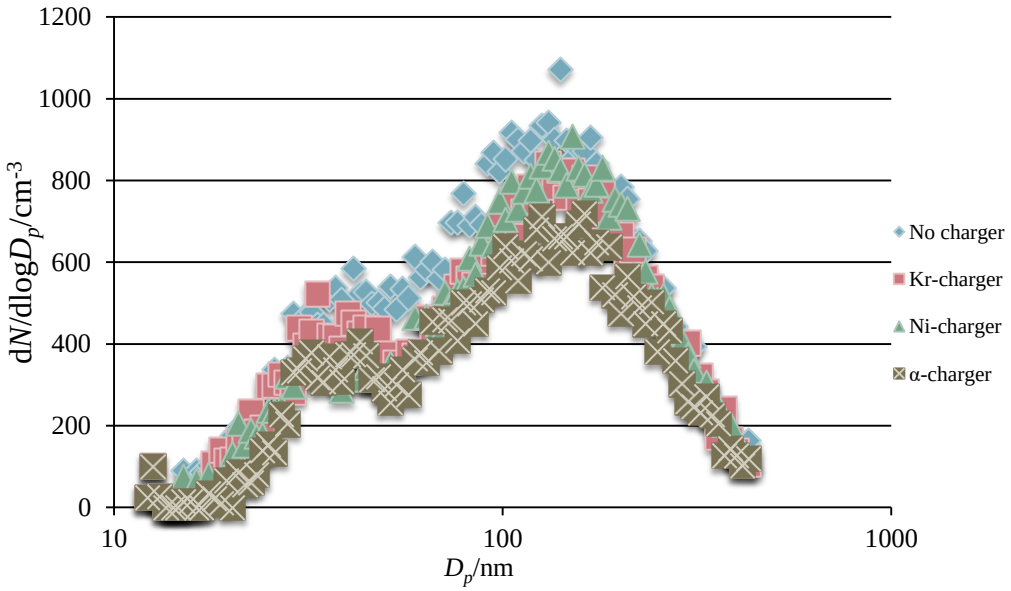

Figure 9a. The first measurement where the α-charger contains 9 Am-sources.

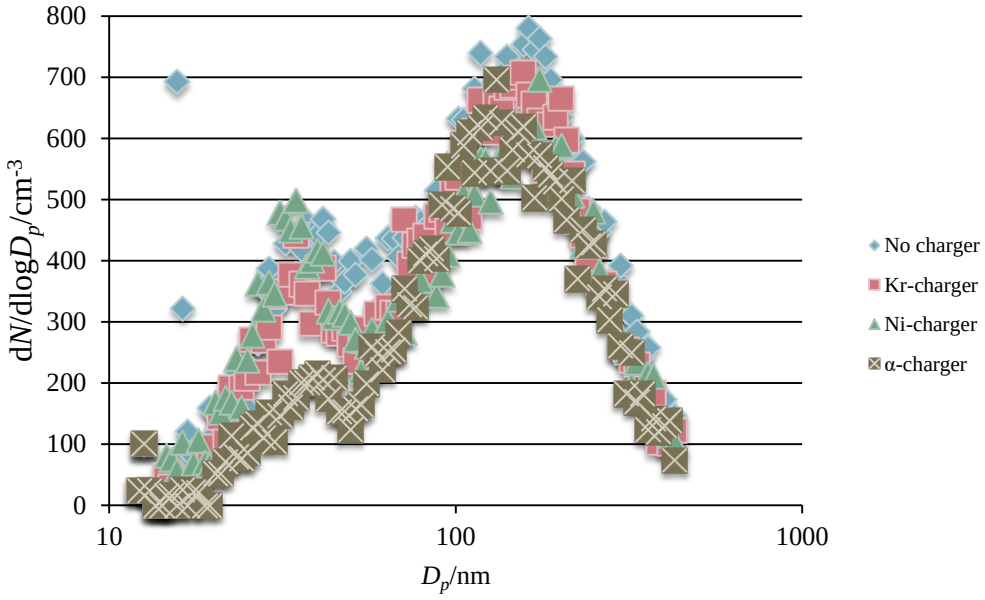

Figure 9b. The second measurement where the α-charger contains 9 Am-sources.

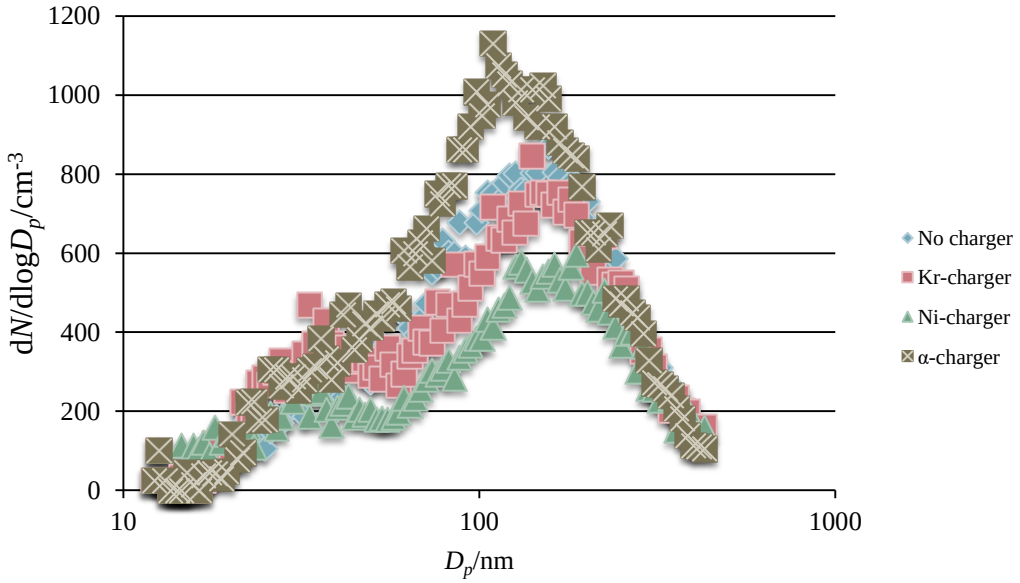

Figure 9c. The third measurement where the α-charger contains 9 Am-sources.

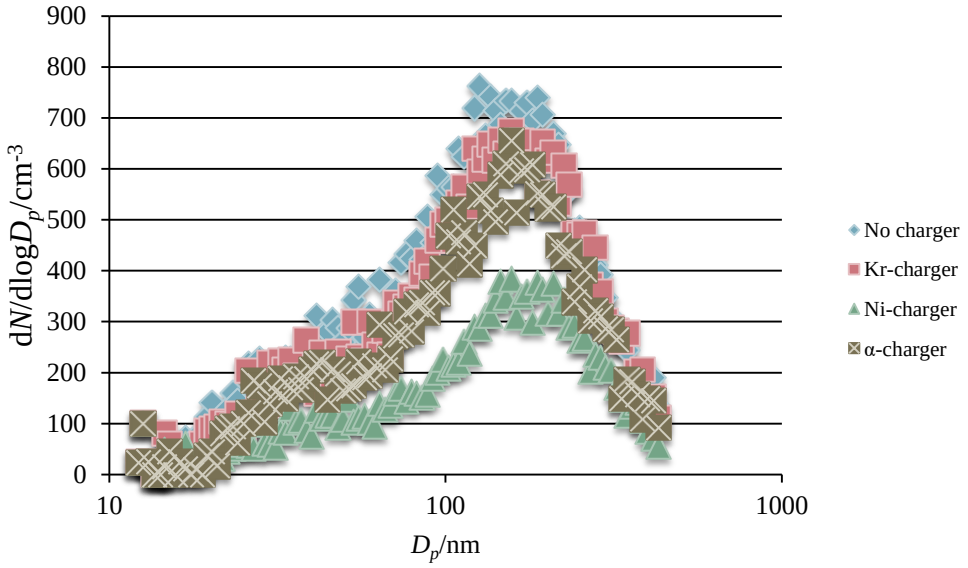

Figure 9d. The forth measurement where the α-charger contains 9 Am-sources.

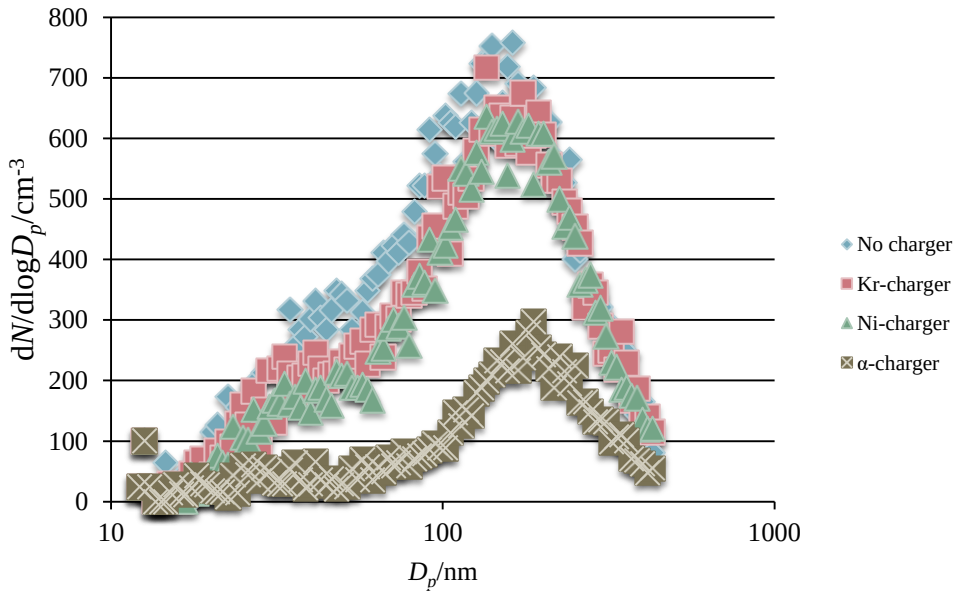

Figure 9e. The fifth measurement where the α-charger contains 9 Am-sources.

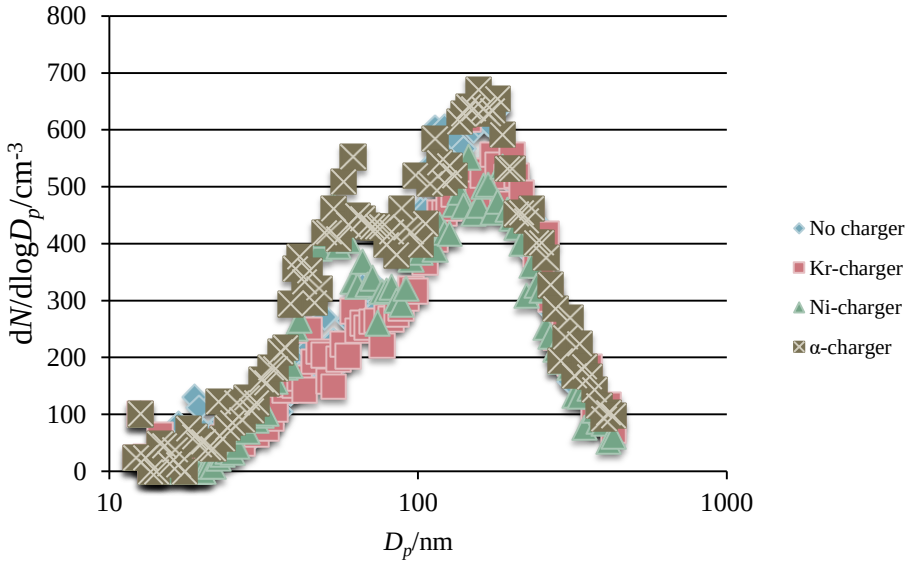

Figure 9f. The sixth measurement where the α-charger contains 9 Am-sources.

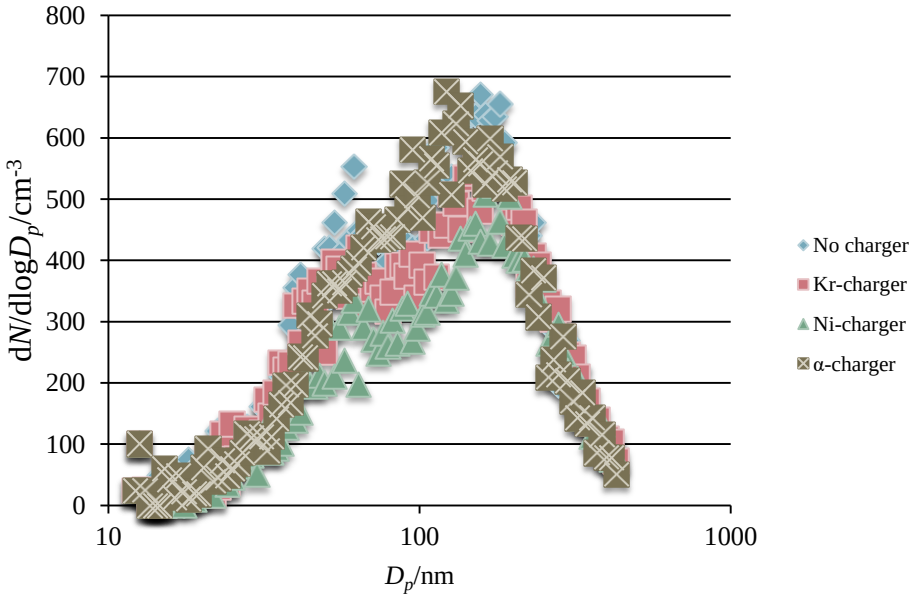

Figure 9g. The seventh measurement where the α-charger contains 9 Am-sources.

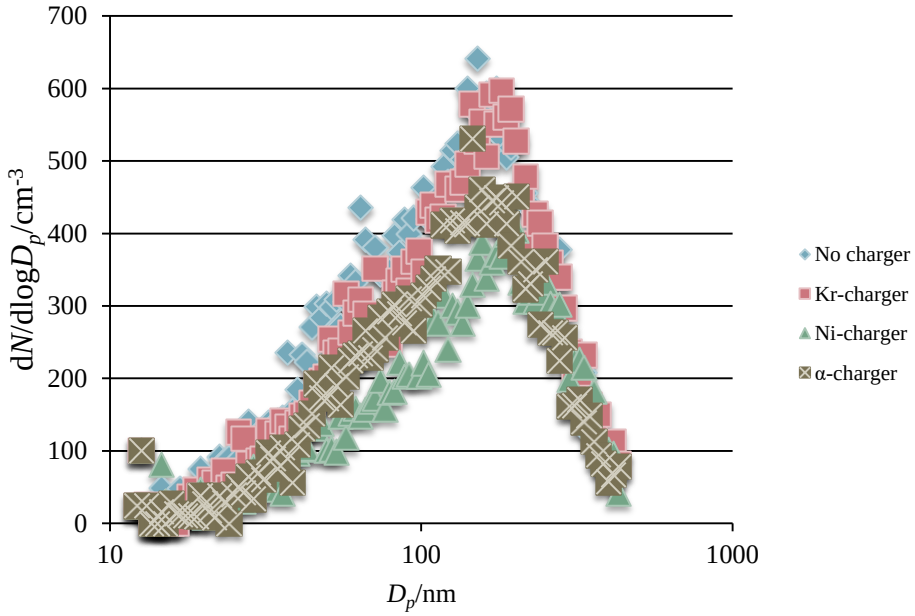

Figure 9h. The eight measurement where the α-charger contains 9 Am-sources.

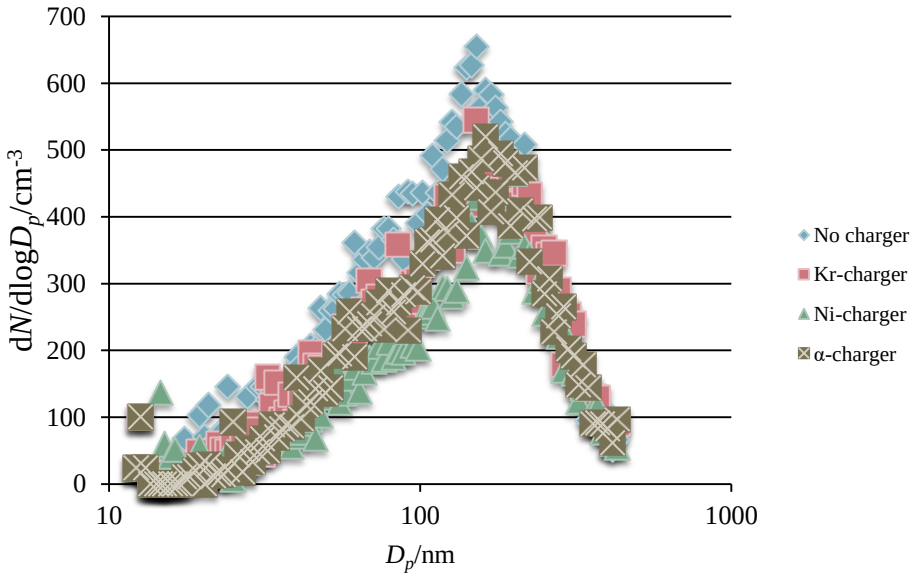

Figure 9i. The ninth measurement where the α-charger contains 9 Am-sources.

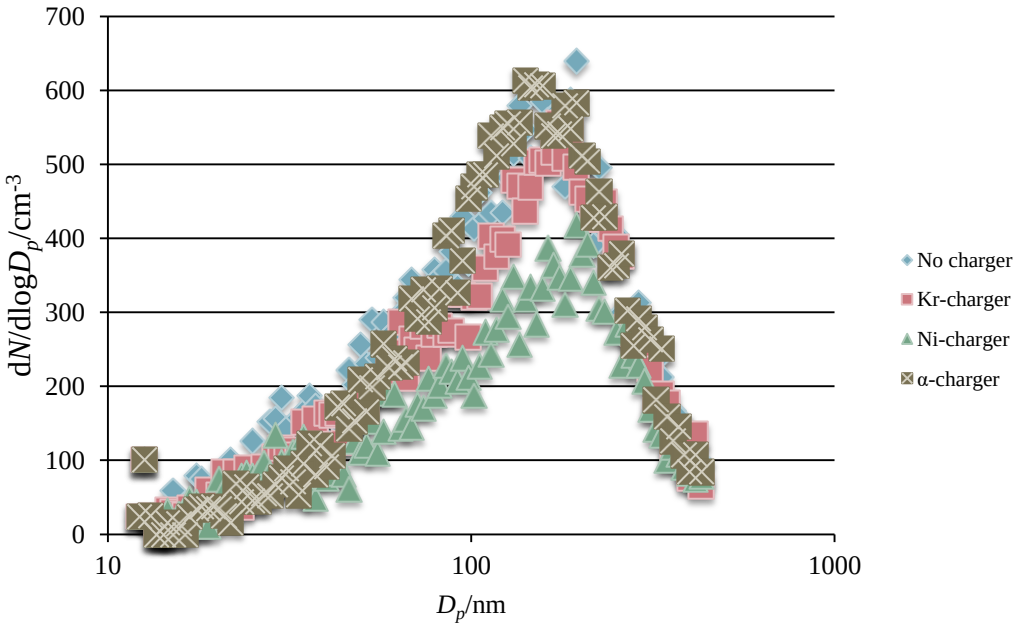

Figure 9j. The tenth measurement where the α-charger contains 9 Am-sources.

Attachment 4 – 15 Am-sources

Attachment 4 presents the measured particle number size distribution for the 10 measurements with 15 Am-sources in the 4 step measurement sequence

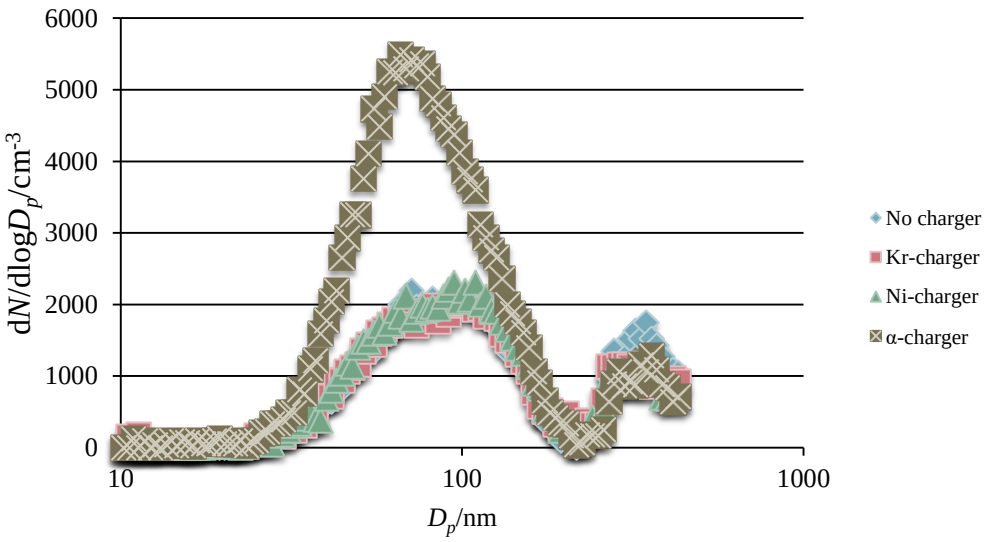

Figure 15a. The first measurement where the α-charger contains 15 Am-sources.

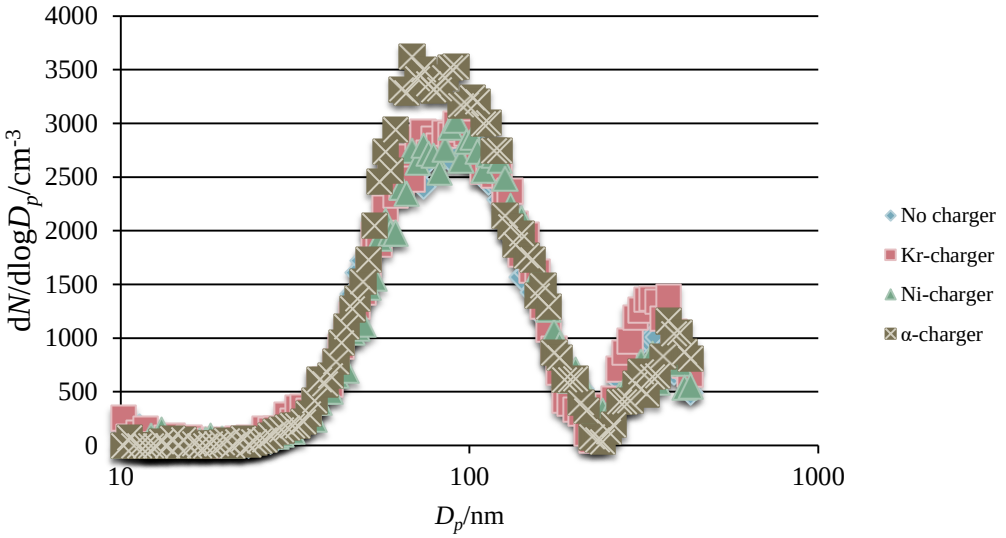

Figure 15b. The second measurement where the α-charger contains 15 Am-sources.

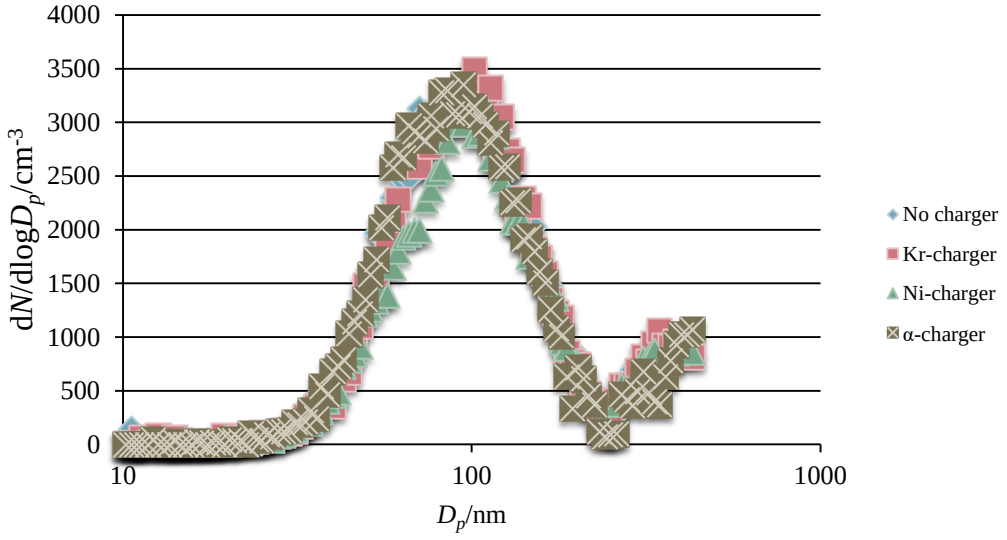

Figure 15c. The third measurement where the α-charger contains 15 Am-sources.

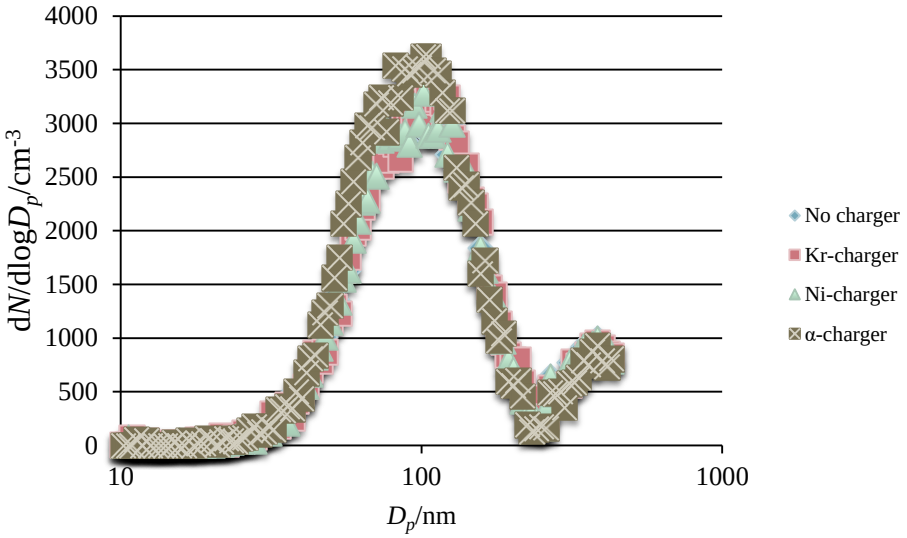

Figure 15d. The forth measurement where the α-charger contains 15 Am-sources.

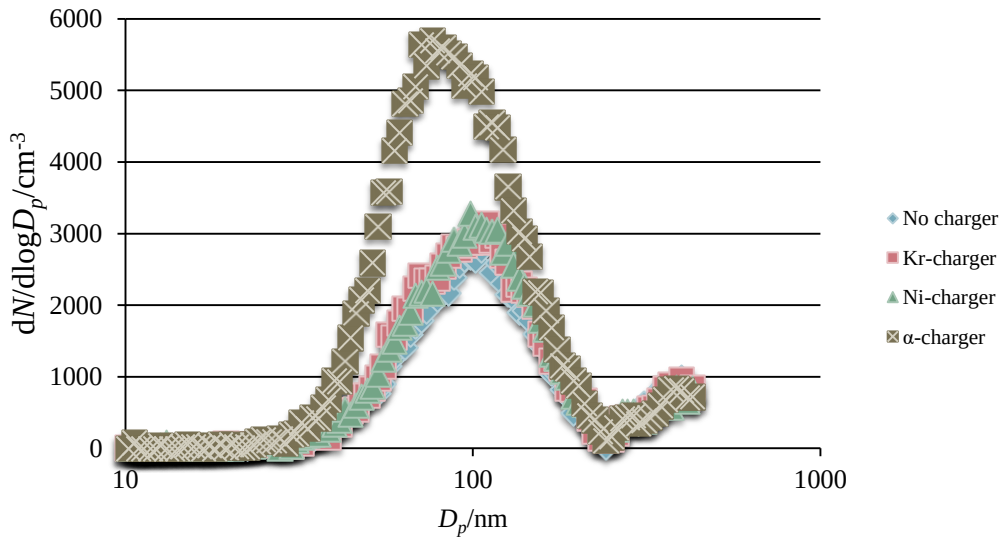

Figure 15e. The fifth measurement where the α-charger contains 15 Am-sources.

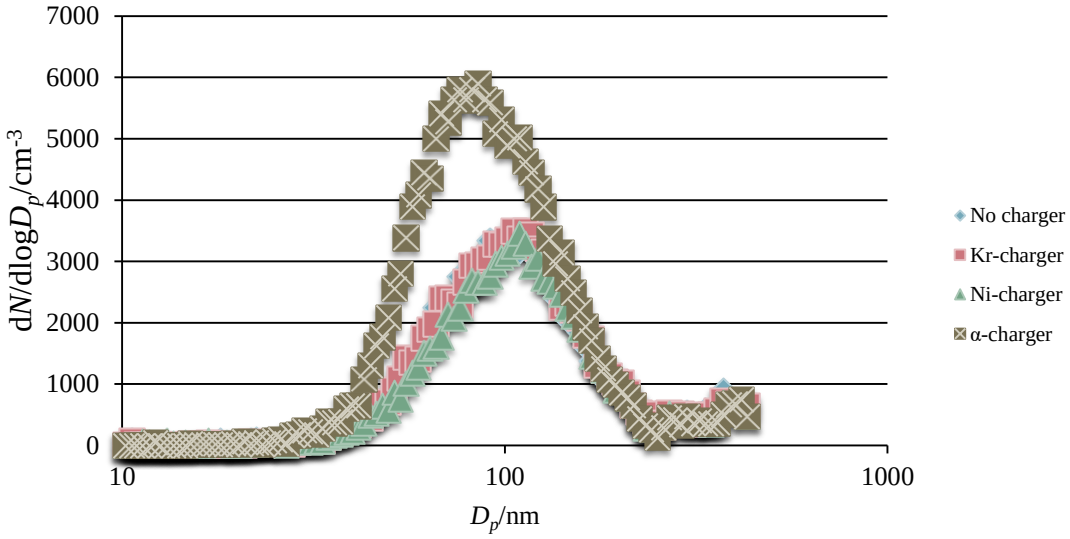

Figure 15f. The sixth measurement where the α-charger contains 15 Am-sources.

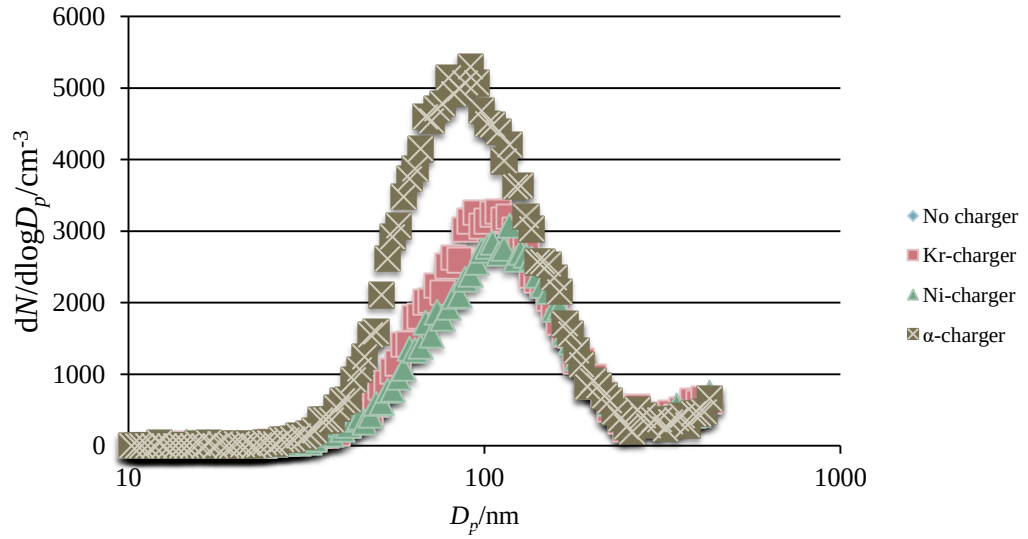

Figure 15g. The seventh measurement where the α-charger contains 15 Am-sources.